PAVOL JOZEF ŠAFÁRIK UNIVERSITY IN KOŠICE
FACULTY OF SCIENCE

INDOOR LOCALISATION USING SMARTPHONES

Dissertation thesis

2020 RNDr. Miroslav Opiela

PAVOL JOZEF ŠAFÁRIK UNIVERSITY IN KOŠICE
FACULTY OF SCIENCE

INDOOR LOCALISATION USING SMARTPHONES

Dissertation thesis

Study Programme:	Informatics
Study Field:	9.2.1. Informatics
Institute:	Institute of Computer Science
Supervisor:	prof. RNDr. Gabriel Semanišin, PhD.
Consultant:	RNDr. František Galčík, PhD.

Košice 2020 **RNDr. Miroslav Opiela**

Univerzita P. J. Šafárika v Košiciach
Prírodovedecká fakulta

ZADANIE ZÁVEREČNEJ PRÁCE

Meno a priezvisko študenta: RNDr. Miroslav Opiela
Študijný program: Informatika (Jednoodborové štúdium, doktorandské III. st., denná forma)
Študijný odbor: Informatika
Typ záverečnej práce: Dizertačná práca
Jazyk záverečnej práce: anglický
Sekundárny jazyk: slovenský

Názov: Indoor Localisation using Smartphones

Názov SK: Indoor lokalizácia s využitím smartfónov

Cieľ:
1. Investigate different aspects of comprehensive localization in buildings with multiple floors.
2. Analyze and compare different Bayesian filtering methods applied on the position estimation.
3. Examine the fusion of the Bayesian filtering with other input data, e.g. map model, Wi-Fi localization.
4. Evaluate proposed indoor localization methods with the focus on the localization accuracy.

Literatúra:
1. Arulampalam, M. S., Maskell, S., Gordon, N., & Clapp, T. (2002). A tutorial on particle filters for online nonlinear/non-Gaussian Bayesian tracking. IEEE Transactions on signal processing, 50(2), 174-188.
2. Šimandl, M., Královec, J., & Söderström, T. (2006). Advanced point-mass method for nonlinear state estimation. Automatica, 42(7), 1133-1145.
3. Chen, Z. (2003). Bayesian filtering: From Kalman filters to particle filters, and beyond. Statistics, 182(1), 1-69.
4. Radu, V., & Marina, M. K. (2013, October). Himloc: Indoor smartphone localization via activity aware pedestrian dead reckoning with selective crowdsourced wifi fingerprinting. In Indoor Positioning and Indoor Navigation (IPIN), 2013 International Conference on (pp. 1-10). IEEE.

Školiteľ: prof. RNDr. Gabriel Semanišin, PhD.
Ústav : ÚINF - Ústav informatiky
Riaditeľ ústavu: RNDr. Ondrej Krídlo, PhD.

Dátum schválenia: 01.09.2015

Acknowledgement

I would like to thank Gabriel Semanišin for the supervising and advices on the PhD study, František Galčík for introducing the field of indoor positioning and the collaboration on the research, my supervised bachelor students for their contribution, my family for support, and IPIN community (organisators of competitions and competitors) for the opportunity to evaluate my approach and for inspiring ideas.

Abstract

The thesis is devoted to the indoor positioning as the essential part of the indoor navigation. Various methods are discussed with the focus on the smartphone-based approaches. The proposed solution combines measurements from the embedded sensors as detected steps and the map model. The inaccuracy is introduced by various factors including noisy measurements and inaccurate step length model. Bayesian filters probabilistically estimate the current position. Various grid-based implementations are proposed in this thesis including the adaptation of the advanced point-mass filter. The solution is evaluated in three buildings - the faculty building in Slovakia, the shopping mall in France, and the research institute in Italy. Datasets and sensor measurements from IPIN 2018 and IPIN 2019 competitions are used for the evaluation and comparison of selected methods. The results, recommended parameter configurations, advantages, main drawbacks, and possibilities for improvement are discussed in the thesis.

Keywords: *Indoor Localisation, Pedestrian Dead Reckoning, Bayes Filters, Grid-Based Filter.*

Abstrakt

Práca je venovaná lokalizácii používateľa v budove ako podstatnej súčasti indoor navigácie. Diskutované sú rôzne metódy so zameraním na tie prístupy, ktoré využívajú smartfóny. Navrhnuté riešenie kombinuje merania zo zabudovaných senzorov vo forme detegovaných krokov s modelom mapy. Nepresnosti sú spôsobené viacerými faktormi vrátane zašumených meraní a nepresného modelu dĺžky kroku. Bayesovské filtre odhadujú aktuálnu pozíciu s využitím pravdepodobností. V práci sú rozoberané rozličné implementácie založené na mriežke vrátane prispôsobenia APM filtra. Riešenie je overené v troch budovách - budova fakulty na Slovensku, obchodný dom vo Francúzsku a výskumný inštitút v Taliansku. Údaje zo senzorov zo súťaží IPIN 2018 a IPIN 2019 sú použité na evaluáciu a porovnanie vybraných metód. V práci sú diskutované výsledky, odporúčané nastavenia parametrov, výhody a nevýhody jednotlivých prístupov a možnosti na zlepšenie.

Kľúčové slová: *Indoor lokalizácia, Detekcia krokov, Bayesove filtre, Mriežkový filter.*

Contents

Acronyms and Abbreviations

APM	Advanced Point-Mass Filter
BLE	Bluetooth Low Energy
CDF	Cumulative Density Function
CNN	Convolutional Neural Network
e. g.	exempli gratia (Lat.), for example, for instance
GF	Grid Filter
GNSS	Global Navigation Satellite System
GPS	Global Positioning System
i. e.	id est (Lat.), that is, in other words
IMU	Inertial Measurement Unit
IPIN	Indoor Positioning and Indoor Navigation (conference)
LSTM	Long Short-Term Memory
PDF	Probability Density Function
PDR	Pedestrian Dead Reckoning
PF	Particle Filter
RFID	Radio-Frequency Identification
RMS	Root Mean Square
RSS	Received Signal Strength
SD	Standard Deviation
SLAM	Simultaneous Localisation and Mapping
ToA	Time of Arrival
TDoA	Time Difference of Arrival
UWB	Ultra-Wideband
VLC	Visual Light Communication
ZUPT	Zero Velocity Update

Introduction

Outdoor positioning based on the GNSS (Global Navigation Satellite System) signal is widely used in various situations. In general, the GNSS signal is not available indoors. Moreover, the positioning system requirements are higher for the localisation in buildings in terms of accuracy. At least 2.5D localisation (with additional information regarding the current floor) is needed in most buildings compared to the outdoor localisation. No universal solution exists for the indoor positioning yet. The indoor positioning and navigation attract many people from academia and industry. Multiple use cases and conditions result in multiple methods with different priorities in the positioning. The activity in the field of indoor navigation and localisation suggests that the most suitable approaches are based on the sensor fusion instead on the only source of information.

This thesis is devoted to the smartphone-based positioning utilizing the smartphone sensors and the map model with the research focus on the grid-based implementations of the Bayesian filtering. The aims of this thesis were derived from the project of the dissertation as follows:

1. Investigate different aspects of comprehensive localisation in buildings with multiple floors.

2. Analyze and compare different Bayesian filtering methods applied on the position estimation.

3. Examine the fusion of the Bayesian filtering with other input data, e.g. map model, Wi-Fi localisation.

4. Evaluate proposed indoor localisation methods with the focus on the localisation accuracy.

In the author's master thesis [1], the grid-based approach was applied on the indoor positioning. The dissemination of the results with an additional evaluation [2] and the comparison with other solutions, mostly using the particle filter or the Kalman filter, stimulated the research of these Bayesian filtering implementations. Various versions of

the proposed grid-based approach were implemented and compared with the particle filter [3] on different scenarios. The research was focused on the best configurations of proposed filters and the overall accuracy using the introduced system with alternating Bayesian filter implementations. Moreover, the advanced point-mass filter combining advantages of grid-based methods and the particle filter was elaborated [4].

The research was supplemented by custom tools for a building map processing, a localisation path visualisation and a simulation of different configurations and methods on the same sensors recordings. The applicability of the introduced approach was evaluated in three buildings - a faculty building in Slovakia with custom path, known subjects, and devices to verify basic concepts and method features. A realistic scenario has been set in a shopping mall in France during the on-site track of the IPIN competition 2018 [5] and using a dataset provided by competition organizers. Another building for the evaluation was a research institute in Italy during the on-site and off-site tracks of the IPIN competition 2019 [6] and using their dataset as well.

Other aspects of the comprehensive indoor positioning and navigation were explored also in bachelor theses supervised by the author of the dissertation. These theses were devoted to the floor transition detection using elevators [7], the visualisation of the navigation path using augmented reality [8], the user activity recognition based on the sensor measurements [9], features and configurations of the particle filter [10], and the navigation path construction including process of creating the map model [11].

The thesis is organized as follows. Chapter 1 introduces the indoor navigation and provides a brief overview of use cases, standards, navigation aspect, and related work. Smartphone sensors useful for the indoor localisation are discussed in this chapter. Chapter 2 focuses on the indoor positioning. Various methods are referenced and the chapter is concluded with the positioning system proposal with basic overview of all considered modules. In Chapter 3, a general definition of the Bayesian filtering is introduced. Various filter implementations, e.g., the Kalman filter or the particle filter, are listed with their definitions, alternations, and research examples using these filters. Chapter 4 introduces five different versions of the grid-based filters. The grid design, the convolution mask computation, the parameter configuration, and the fusion with inputs from other sources (e.g., Wi-Fi) are investigated. In Chapter 5, the evaluation of all grid-based methods and the particle filter is presented. The general overview of the methodology, venues and scenarios is included in this chapter. Results based on the custom evaluation, IPIN competitions, and provided datasets are summarized and the thesis is concluded with lessons learned from the competitions and evaluation in realistic scenarios.

1 Indoor Navigation Applications

The focus of this thesis is on the indoor positioning system. However, all proposed methods were elaborated with the goal to be a part of the navigation application. The positioning system is the essential component of every navigation application. Nevertheless, other features (including the navigation path and visualisation) are important for the usable application. Various aspects of navigation and positioning applications are discussed.

1.1 Definitions, Attributes, Benchmarking

Indoor positioning systems have been studied in the past decade and various researchers, companies, and institutions are still active in introducing new approaches for various use cases. Moreover, some effort has been taken to address the open challenges such as the standardisation, evaluation, benchmarking, etc. As an example, Furfari et al. [12] attempted to define missing features of the positioning system as protocols, services, and taxonomies. The first formal definition of a methodology for the evaluation is the ISO/IEC 18305:2016[1] international standard. Potorti et al. [13] reviewed the standard and confronted it with current evaluation activities that the community has been doing in the form of indoor positioning competitions.

In the standard, positioning and localisation are distinguished. If an entity (object, person, robot) needs to know its own position, it is called positioning. However, if this position is needed to be known by another entity, it is denoted as localisation. However, the standard adopted the term localisation for both situations. The positioning method is the aim of this thesis but these terms are exchangeable for this case. Standards defines scenarios and five types of buildings (single-family house, office building, warehouse, high-rise steel, subterranean) for the complex evaluation of a positioning system.

The standard recommends to use the black box evaluation, i.e., without any knowledge of its inner processes and modules. The solution should be tested on the system

[1] ISO/IEC 18305:2016 Information technology — Real time locating systems — Test and evaluation of localisation and tracking systems. https://www.iso.org/standard/62090.html

level by considering the localisation output. In the standard, parameters are defined for such evaluation, e.g., the number and the density of testing points. A few competitions were organised for the evaluation of systems developed by competitors. Microsoft indoor localisation competition was launched as a part of international conferences on Information Processing in Sensor Networks (IPSN) [14]. The conference on Indoor Positioning and Indoor Navigation (IPIN) launched the competition using so-called EvAAL framework [15]. The system proposed in this thesis was evaluated on two IPIN competitions. The considered metrics at these competitions is the Euclidean distance between the checkpoint true position and the estimated location with the penalty for the misdetected floor. Various track are available at the competition, e.g., IPIN 2019 included smartphone-based and video-based on-site tracks and smartphone-based, foot-mounted IMU (Inertial Measurement Unit) based, and xDR in industrial scenarios off-site tracks.

Other approaches to rate the positioning accuracy are possible. Villien et al. [16] defined perfect, good, middle, and bad performance based on the percentage of time when the error is under 5 meters. Mendoza-Silva et al. [17] introduced a method measuring the error as the length of the pedestrian path connecting estimated positions with the true positions. The pathfinding is applied using various approaches for vector and raster maps.

A list of user requirements is introduced by Mautz [18]. Moreover, Al-Ammar et al. [19] in their comparative survey of positioning algorithms and technologies included also performance metrics list. Besides the accuracy, other attributes are also important to address in the application of indoor navigation and localisation. Holcer et al. [20] introduced a systematic review of the privacy in indoor positioning systems. Barsocchi et al. [21] proposed a privacy-by-design architecture of the system. Another important factor of the deployed application is the cost which includes the time and money required for the infrastructure installation, maintenance, and possibly the device costs. Energy consumed by devices should be considered for the system, e.g., passive RFID (radio-frequency identification) tags, BLE (Bluetooth Low Energy) beacons powered by batteries. Scalability, availability, and coverage area influence the number of user able to be localised at the same time and the overall experience using the positioning system.

1.2 Use Cases, Navigation, Related Work

The field of indoor positioning and indoor navigation is not unified. Various conditions, buildings, users, and situations declared priorities for the positioning system. A few examples of use cases are listed as follows:

- pedestrian navigation in a building complex [22],
- visually impaired visitors in a museum [23],
- patients searching for a hospital ward [24],
- drone navigation in a warehouse [25],
- person on a wheelchair navigation [26],
- positioning in a historical building [27],
- car navigation in a parking garage [28],
- positioning and navigation of firefighters in unknown buildings [29].

Multiple attributes are important for these use cases. The navigation of impaired visitors and firefighters require high reliability. The system for firefighters should also satisfy the minimal set-up time request and the resilience due to the emergency scenario. The drone navigation demands on the high accuracy. Common pedestrian navigation may tolerate lower accuracy but the user experience with the navigation is determining the success of the proposed solution (e.g., the clearness of navigation signs, path choice on junctions). The installation of additional infrastructure may be not allowed in some types of buildings (e.g., historical buildings) or too expensive in large environments.

Problems related to the navigation are the map model construction, the path finding, and the visualisation. Lin et al. [30] proposed a mapping solution for 3D indoor spaces extended with the grid tessellation and the pathfinding. The fast marching method was applied for tracking the shortest path with addition of the semantic building representation to avoid obstacles. The fast marching method outperformed ant colony and A* algorithms. Zhou et al. [31] introduced a pathfinding method (based on breadth-first search and Dijkstra's algorithm) applied on the grid-topological map. The grid is generated using geometric and semantic data and the topological map as a skeleton is constructed using a grid thinning approach. Li et al. [32] introduced a survey on map standards and formats. Indoor OSM, IndoorGML, IFC, and CityGML are listed as relevant map models with the discussion regarding 2D vs. 3D, the geometry, the expressive power, and the efficiency. These tools are mostly based on XML format. Besides the manual map model creation, the mapping procedure may be performed using LIDAR-based systems, the vision-based methods (e.g., using the common camera and the depth camera by Microsoft Kinect), and the smartphone SLAM (simultaneous localisation and mapping) technique. Pipelidis et al. [33] proposed a vertical mapping system based on the crowdsourcing.

Augmented reality is the popular technology in the smartphones with wide range of applications. The camera image extended with navigation signs (arrows or highlighted paths) may improve the user experience using the navigation application. The combination of the augmented reality and the indoor navigation is addressed in various publications, e.g., [34], [35], [36].

1.3 Smartphones and Sensors

The success of the indoor navigation application depends on various factors. The user device, the use case and the building type should be recognized. It may be convenient for the shopping cart navigation to install specific sensors or devices or lending the device for museum visitors similar to audio guides in some such institutions. Petrelli and O'Brian [37] declared the preference of museum visitors for tangible interactions (e.g., smart cards, smart replicas) over a phone application. Moreover, visitors expected museum to provide these phones. However, the navigation in public building with occasional visitors, e.g., shopping malls or airports, should not insist on any extra devices for the user. Ubiquitous smartphones with inertial sensors represent an opportunity for widely deployable solutions according to the *bring your own device* approach.

Callebaut et al. [38] commented on the absence of studies dedicated to smartphone sensors and challenges related to the implementations of sensing applications. They declare the satisfactory accuracy in the sensor sampling frequency (evaluated for the accelerometer) and discuss techniques to avoid data loss due to the processor sleep mode. One of the main challenges considering smartphones is the noise and sensors accuracy. Stisen et al. [39] evaluated the accelerometer in 36 smartphones and smartwatches. The average offset deviations were between 0.74 ms^{-2} to 0.83 ms^{-2} and the biases accross all devices were indicated as a near normal distribution with a mean 9.76 ms^{-2}. Li et al. [40] observed the average error in the heading obtained from sensors at 12° with the 95th percentile at 32° and the maximum at 40°. Blum et al. [41] declared the mean of the compass error between 10° and 30° but with the high standard deviation making it unreliable.

Smartphone sensors are available to a developer as virtual sensors which derive their values from physical sensors. Sometimes these measurements may be processed or obtained from multiple sensors. In this thesis, the Android operating system is preferred due to its market share and the developer tools for sensor measurements. A few relevant sensors and smartphone modules are listed as follows:

Accelerometer

The three-axes accelerometer is available in almost every smartphone and it me-

asures the acceleration force along the axes including the gravity. According to the Android documentation[2], it consumes about 10 time less power than other motion sensors. It is possible to detect a movement of a user (tilt, shake, rotation, swing) and hence to detect the performed step. It is recommended to apply low-pass and high-pass filters to reduce the noise.

Gyroscope

The three-axes gyroscope measures the rate of rotation along the axes using the same coordinate system as the accelerometer. Typically, the gyroscope is used in combination with other sensors for particular tasks of the indoor positioning.

Magnetometer

The geomagnetic field sensor allows to determine the position of a device. The smartphone orientation is computed from magnetometer values along with the acceleration measurements. Moreover, the magnetometer sensor may be utilized for other aspects of the indoor positioning, e.g., the initial position estimation or the fingerprinting map, since it is not restricted to observe only relative movement of the device.

Barometer

The measurements of the ambient air pressure obtained from the barometer sensor are useful for the vertical localisation. It is possible to calculate the current altitude but other parameters (pressure at sea level, air temperature) are needed. Moreover, the accuracy of such approach without any external reference is questionable. Nevertheless, the relative change in the pressure values is applicable for the floor transition detection.

Pedometer

It is possible to detect or count steps based on the accelerometer. It is available as a software sensor for the step counting and detection in Android. The counting provides results with higher accuracy in exchange for the more latency compared to the step detection. There were attempts to add a hardware chip (e.g., Google Nexus 5) for the step detection which is no further present in smartphones.

Light

The light sensor measures the level of illuminance in lux units with the possible usage in indoor-outdoor transition detection or positioning approaches based on the luminaries in the building [42].

[2]Motion sensors — Android documentation. https://developer.android.com/guide/topics/sensors/sensors_motion.html

GNSS

The GNSS signal is mostly not available indoors. However, in some situations it may be used for occasional position estimation, e.g., to identify the entry point to the building or in the top floor in a shopping mall with a glass roof.

Wi-Fi

The benefit of existing Wi-Fi infrastructure in buildings is popular for the positioning using techniques of lateration or fingerprinting. The scanning of Wi-Fi available access points and the strength of signals is the essential component in such localisation approaches. However, the Wi-Fi throttling[3] was introduced to improve network performance and battery life. Since Android 8, a background application may scan Wi-Fi networks only once per 30 minutes. Android 9 extended it with the limit of 4 scans per 2 minutes for foreground applications. In Android 10, it is possible to turn off the throttling for local testing in developer options.

Bluetooth

Positioning based on beacons provides some advantages over Wi-Fi even though the installation and maintenance of the infrastructure is required. The battery-powered beacons operate using the Bluetooth 4.0 Low Energy standard (BLE). BLE transmitters broadcast their identifiers to available devices including smartphones.

UWB chip

Ultra-wideband technology approaches are present in the field of indoor positioning already achieving high accuracy. The first smartphone with the UWB chip was iPhone 11 and currently the only Android-driven smartphone with the chip is Samsung Galaxy Note 20 Ultra, but new models with the UWB chip are expected.

Camera

Various approaches utilize the camera image or recording for the positioning. The main difference compared to a robot positioning is that the camera is not in the fixed position but the smartphone is moving mostly in hand. There are smartphones with multiple cameras (e.g., Samsung Galaxy S20) or even with the depth sensor (e.g., Lenovo Phab 2 Pro). The depth camera is not available generally, but opens possibilities for mapping applications or the augmented reality.

[3] Wi-Fi scanning overview - Android documentation https://developer.android.com/guide/topics/connectivity/wifi-scan

2 Comprehensive Indoor Positioning

Various techniques are applied to position a user, a robot, or other devices in the indoor environment. These methods achieve different levels of accuracy. Initial costs, severity of the deployment and the maintenance, available infrastructure, and the use case may suppress some methods to be widely used for the indoor localisation. Mendoza-Silva et al. [43] introduced an extensive review of the current state in the indoor positioning field with references to other surveys and relevant work for particular localisation approaches. Davidson and Piche [44] provided an overview of positioning techniques focused on smartphones. The most relevant approaches to our use case are introduced and the applied positioning system is proposed in this thesis.

2.1 Radio Frequency Indoor Localisation

One category of localisation methods is based on the system where the device is a receiver of a signal. Besides the method using pseudolites to transmit signals detectable by GPS (Global Positioning System) receivers [45], a few types of approaches are applicable in this scenario. Most common methods are based on the distance calculation to the emitters, e.g., time of arrival (ToA) method computes the distance by measuring the time needed for a signal to arrive from the transmitted with known speed. Similar method TDoA (time difference of arrival) measures differences in time of arrived signal from different transmitters. The RSS-based methods (received signal strength) measure the intensity of the signal strength as the strength is decreasing with the distance. Tariq et al. [46] devoted a survey to non-GPS positioning techniques. Technologies suitable for the RSS approach are listed as UWB (ultra-wideband), RFID, Bluetooth, magnetic field, cellular networks, wireless network, and VLC (visual light communication). Besides the aforementioned approaches and pedestrian dead reckoning (PDR), the survey discussed other approaches, e.g., roundtrip time of flight, received signal phase method, angle of arrival. Moreover, range-free methods exist which does not measure the received signal, i.e., hop count approach for coarse positioning based on the hop detecting when a packet passes from a network segment to another.

The positioning method using the aforementioned approaches is based on geometric methods of lateration or angulation. The trilateration (or the multilateration, depending on the number of available signal from transmitters) utilizes the distance and the triangulation (or multiangulation) approach uses the direction of the signal. Villien et al. [16] performed experiments where the logarithmic model was expected for the distance calculation based on the Wi-Fi signal. However, the evaluation revealed the linearity and suggested to use two linear models based on the distances greater than 35 m and smaller values. Torres-Sospedra et al. [47] discussed that the logarithmic nature of the Wi-Fi signal is mostly not considered in related approaches.

Large buildings require more transmitters for the localisation and the effort to obtain the position of the devices may be too excessive. The popular method for the localisation is the fingerprinting. The offline stage of this method is based on the fingerprint collection construction. Fingerprints are created for specific positions where the list of available transmitters with the signal strengths is scanned and stored. The positioning is performed by retrieving the respective fingerprint for the characterization of the current real position based on the obtained signal strengths. If signals are radio frequencies, the acquired database is called radio map.

The offline stage of the fingerprinting may be performed using crowdsourcing, i.e., the group of users contributes to the overall knowledge. Rai et al. [48] applied this approach to obtain measurements without any explicit effort from the user. Moreover, the initial position estimation is selected based on the Wi-Fi fingerprinting method. He and Chen [49] proposed a review of recent advances and comparisons of the Wi-Fi fingerprinting positioning. Practical aspects of such solutions, efficient deployment, advanced techniques, and future directions are addressed. Khalajmehrabadi et al. [50] discussed three main approaches to the fingerprinting, i.e., deterministic, probabilistic, and machine learning. Kriz et al. [51] extended existing Wi-Fi infrastructure with iBeacons and achieved improved accuracy. Wi-Fi throttling, energy demands for Wi-Fi scans, and other drawbacks supports applications based on BLE. Karmacharya et al. [52] proposed a localisation method using BLE. The results demonstrate the improvement of the positioning accuracy with the fusion of such method with measurements obtained from inertial sensors. Another technology for the positioning is based on UWB achieving better performance compared to other methods, even though it is currently commercially expensive solution. Alarifi et al. [53] discussed the UWB-based positioning in their survey.

2.2 Pedestrian Dead Reckoning

The PDR utilizes sensors to detect the movement of a user for the position estimation. When a step is detected, the transition is performed as follows:

$$\mathbf{position}_t = \mathbf{position}_{t-1} + L_t \Big[sin(\theta_t), cos(\theta_t) \Big]^T, \tag{1}$$

where L_t is the step length and θ_t is the step bearing obtained at time k. Particular tasks associated to the PDR are step detection, step heading calculation, step length estimation, and initial position determination. The PDR computes relative position based on the previous estimation. Another source of information is required to start the process and fusion with other approaches may reduce the drift or the accumulative error which is increasing in time. Solin et al. [54] initialized the solution based on the first magnetometer reading which converged to a satisfactory estimation within a few seconds. The Bayesian filtering technique is typically applied to deal with the uncertainty and faulty PDR outputs. It is possible to initialize the filter at random positions with equal weights across the map [55] and utilize the map model to obtain the true position during the process.

Numerous related publications are devoted to the pedestrian dead reckoning using inertial measurement units. The IMU is a device containing the accelerometer, the magnetometer, and the gyroscope. This device may be fixed on a user foot [40], belt [56], shoe [57], or elsewhere. The foot mounted IMU are the most suitable for the step detection utilizing the stance phase of a step with no movement of the device and the foot. Periodic zero velocity updates (ZUPT) are performed to bound the error [58].

Nevertheless, the smartphone-driven PDR is derived from the IMU-based reckoning but some of particular methods are adjusted for the different type of device and the movement style (handheld smartphone). Bergmann and Hou [59] introduced a systematic review of PDR approaches with wearable sensors and Wu et al. [60] summarized the research status of PDR using inertial sensors.

Step detection

Zero velocity approach is typical for foot mounted IMU. Zhang et al. [61] introduced the Markov model method and described the walking motion using four states. Satisfactory results are obtained using various methods. Brajdic and Harle [62] evaluated the step detection methods considering various smartphone placements and declared the fact that no algorithm was 100% reliable. Lee et al. [63] achieved accuracy over 98% for various combinations of step modes and device poses. Link et al. [64] detected steps based on the accelerometer values when the

current measurement decreases significantly. Moreover, the timeout value prevents false steps to be detected as it is not possible to perform more steps in within the timeout. Radu and Marina [65] applied the zero crossing method on smoothed acceleration measurements. They summarised three main approaches for the step detection on the smartphones. Besides the zero crossing method, the peak detection searching for local maximum or minimum in the acceleration magnitude or autocorrelation leveraging the repetitiveness of human walking are commonly used for the step detection.

Step length

Vezočnik and Juric [66] proposed a survey of step length estimation methods. Thirteen considered approaches were classified to a few categories based on the step frequency, the acceleration, the angle, and multiparameter methods. Most accurate results were obtained using the step frequency approach, especially the solution introduced by Weinberg [67]. However, the overall accuracy may be increased using the calibration for a specific user. The accelerometer-based methods outperformed other approaches using personalized constants, especially the method proposed by Tian et al. [68]. The evaluation included various walking speeds and device placements.

Step heading

The device orientation values may have a drift. Moreover, the metals and electrical equipment have impact on the accuracy [69]. Inaccuracy or drifts may be reduced using more advanced methods, e.g., the Kalman filter [70]. Wu et al. [71] proposed a system based on the Kalman filtering incorporating accelerometer, gyroscope, and magnetometer measurements. The model limits outliers and resists negative effects of the disturbances. Kang et al. [72] introduced the step heading method utilizing the magnetometer and the gyroscope where measurements from these two sensor are combined to suppress the drawbacks of particular sensors. Seo and Laine [73] applied a method to determine the device orientation (before the step detection) to avoid significant errors with changes of the device holding styles.

2.3 Selected Indoor Positioning Methods

Besides the PDR and radio frequency positioning methods, other approaches relevant for this thesis are reviewed. The performance of the proposed system may be improved using additional methods based on the activity recognition, computer vision,

and machine learning. Knowledge of the context or the activity (e.g., standing in an elevator, walking, running) introduces another source of information. Using this knowledge, the position may be adjusted (e.g., the position of a few elevators is known in the building) or other parameters may be adapted (e.g., the step length on stairs is shorted than during the normal walk). Moreover, these approaches are useful also for the comprehensive indoor positioning including vertical localisation.

Even though some systems utilize the Bayesian filtering method for the 3D localisation, e.g., the particle filter solution proposed by Bojja [74], the popular approach is to incorporate a method of the floor transition detection. The detection of such event may serve also as a landmark for the positioning [75]. Xia et al. [76] discussed that the height of floors in buildings is often unknown and installed devices with the barometer for the reference. Various approaches are used for the context recognition. Radu et al. [77] applied the deep learning method for interpreting the user activity and context recognition. Wang et al. [69] introduced a system based on a decision tree, where the elevator is recognized at the top level based on the acceleration measurements. Walking and stairs are separated using the variance in these values. Moreover, the magnetometer supports the recognition of the escalator, stairs, and the stationary. Susi et al. [78] proposed a training-based model for the classification of motion modes. Four categories are considered, i.e., static situations, regular moving (calling, texting, bag carrying), hands winging, and irregular motion.

Regarding the machine learning methods, the LSTM (long short-term memory) neural network (a type of recurrent neural network) is commonly applied and achieving promising results, e.g. [79], [80]. Wang et al. [81] published a survey on deep-learning methods for the activity recognition. One of the most common approach is the convolutional neural network (CNN). Shao et al. [82] utilized the CNN for the classification of the fingerprint images based on Wi-Fi and magnetic field. CNN is also suitable for the computer vision methods. Camera-based tracks are a part of IPIN competitions. Li et al. [83] proposed a system using deep learning technique on consecutive video frames. Duque Domingo et al. [84] integrated the computer vision method with the Wi-Fi localisation. Cooper and Hedge [85] installed low cost webcameras in the building to localise persons.

2.4 Proposed Positioning System

The considered use case is a positioning and navigation of a pedestrian in indoor environment. The first aim is to navigate university students but proposed system is not restricted to this type of building. The user is holding the smartphone and looking

at the screen where the visual information about the location and other navigation features are displayed. The system is based on the floor plans in any format, mostly as a georeferenced image. No additional infrastructure in the building is required.

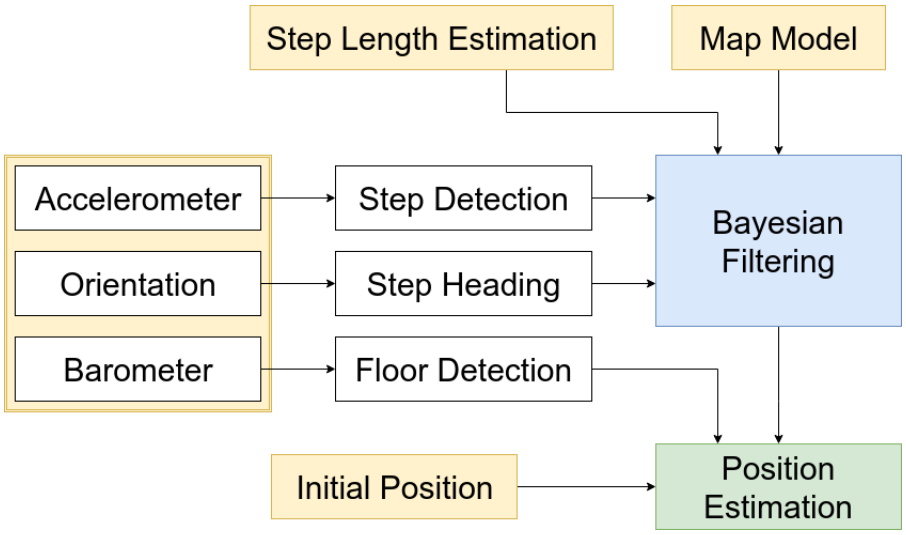

Fig. 1: Overview of the proposed solution. Various implementations are examined for the Bayesian filtering.

Figure 1 describes main modules of the proposed localisation approach:

Sensors

Smartphone equipped with sensors is required for the positioning. The accelerometer is used for the step detection and for the heading calculation in combination with the magnetometer. Moreover, if the gyroscope is available, the performance and the stability may be improved. The barometer is needed for multifloor positioning.

Step detection

Steps are detected using acceleration values. Values from all three axes are combined, low-pass filter is applied for smoothing, and the zero-crossing method is executed to identify performed steps. A step detection initiates the process of a position estimation calculation.

Step heading

The current direction of the user is computed using mostly the accelerometer and the magnetometer through the provided Android developer tools. Values are filtered and inserted into the process of PDR.

Floor detection

Significant relative change in barometer measurements, indicating the floor transition, triggers the reset of positioning system. The map model is loaded for the

current floor, the initial position is selected according to the respective entry point to the floor, and the Bayesian filtering method is restarted. Locations of entry points (e.g., elevators, staircases, etc.) are stored for every floor.

Initial position

Pedestrian dead reckoning calculates the estimated user location based on previous estimations. In the evaluation, the initial position is selected manually. It corresponds to the use case of a user scanning the QR code placed in the building. However, it is more preferable to reduce the requirement of user input or action. Other techniques may be implemented, e.g., the GNSS signal as for the off-site competition in this evaluation.

Step length estimation

The expected step length is assigned for every run, even though there are methods to calculate the value. Experiments were performed to adjust the estimation based on the overall performance resulting as hints to increase or decrease the step length. However, the fixed value (possibly calibrated for a selected user) is considered and the influence of underestimated and overestimated values is elaborated.

Map model

Available floor plans are processed using custom editor similar to common geographic information systems. The walls and available zones are denoted (see Appendix A). A coordinate system with centimeter level accuracy is applied. The map model is stored in a custom format.

Bayesian filtering

The technique models the uncertainty introduced by noisy sensor measurements and inaccurate inputs (e.g., step length or heading). Various implementations are elaborated in this thesis.

Position estimation

The current user position is selected as the place with the highest probability among all considered positions based on the Bayes filter implementation. The new position is calculated when the step or the floor transition is detected.

3 Bayesian Filtering

Z. Chen [86] contributes with the overview of Bayesian Filtering with basic notations, different implementations, and areas of application. Bayes filters are useful in domains of target tracking, computer vision, robotics, speech enhancement and recognition, machine learning, financial and time series analysis, and fault diagnosis. Fox et al. [87] define Bayes filters as filters which probabilistically estimate a state of a dynamic system using noisy measurements obtained up to the current time of the estimation. The technique is suitable for the indoor positioning due to the ability to deal with inaccuracy accumulated by noisy sensors and imperfect methods of the PDR or other components. Moreover, the Bayes filtering may be applied to particular tasks of the indoor positioning, e.g., the step length model calibration [88] or the activity recognition [89]. The notation of the Bayesian filtering and its implementations is in accord with the referenced author's publication [3].

3.1 Formal Definition and Application on Indoor Positioning

The PDR-based indoor positioning system is able to indicate the current state only with limited accuracy. Considering indoor localisation, the state consists of the user position and possibly other parameters, e.g., the velocity or the direction. The filtering models the uncertainty introduced by inertial sensors.

Bayes filters represent the state at the time $k \in \mathbb{N}$ by a multivariate random variable $\mathbf{x}_k$ and a probability distribution over $\mathbf{x}_k$ is called belief. The aim of the filter is to sequentially estimate the conditional probability density function $p(\mathbf{x}_k|\mathbf{z}_{1:k})$ of the state $\mathbf{x}_k$ given the sensor data as measurements $\mathbf{z}_{1:k} = \{\mathbf{z}_i, i = 1, \ldots, k\}$ for the discrete-time stochastic system:

$$\mathbf{x}_k = \mathbf{f}_k(\mathbf{x}_{k-1}) + \mathbf{w}_k, \qquad k = 1, 2, \ldots \tag{2}$$

$$\mathbf{z}_k = \mathbf{h}_k(\mathbf{x}_k) + \mathbf{v}_k, \qquad k = 1, 2, \ldots \tag{3}$$

where $\mathbf{x}_k \in \mathbb{R}^{n_x}$ is a vector representing the system state and $\mathbf{z}_k \in \mathbb{R}^{n_z}$ is a vector representing the measurements at the time k. Vector functions $\mathbf{f}_k : \mathbb{R}^{n_x} \to \mathbb{R}^{n_x}$ and $\mathbf{h}_k : \mathbb{R}^{n_x} \to \mathbb{R}^{n_z}$ are known and $\mathbf{w}_k \in \mathbb{R}^{n_x}$, $\mathbf{v}_k \in \mathbb{R}^{n_z}$ represent known, mutually independent zero-mean state and measurement noise. The solution of the filtering problem is given by the Bayesian recursive relations consisting of two stages - the prediction and the correction:

$$\underbrace{p(\mathbf{x}_k|\mathbf{z}_{1:k-1})}_{\text{prediction}} = \int \underbrace{p(\mathbf{x}_{k-1}|\mathbf{z}_{1:k-1})}_{\text{prior PDF}} \underbrace{p(\mathbf{x}_k|\mathbf{x}_{k-1})}_{\text{transition}} d\mathbf{x}_{k-1} \tag{4}$$

$$\underbrace{p(\mathbf{x}_k|\mathbf{z}_{1:k})}_{\text{correction (posterior PDF)}} = \frac{\overbrace{p(\mathbf{x}_k|\mathbf{z}_{1:k-1})}^{\text{predicted PDF}} \overbrace{p(\mathbf{z}_k|\mathbf{x}_k)}^{\text{evaluation}}}{\underbrace{\int p(\mathbf{x}_k|\mathbf{z}_{1:k-1}) p(\mathbf{z}_k|\mathbf{x}_k) d\mathbf{x}_k}_{\text{normalizing constant}}} \tag{5}$$

At the prediction stage, the probability density function (PDF) is distributed and spread according to the transition model (Equation 2), which brings more uncertainty to the state estimation regarding the noise $\mathbf{w}_k$. For the system state estimation $\mathbf{x}_k$ at the time k, the measurements $\mathbf{z}_{1:t}$ are required. Depending on the available measurements, one can distinguish stochastic smoothing if $t > k$, stochastic prediction given $t < k$ and stochastic filtering problem for $t = k$. Posterior PDF estimation is computed from the prior PDF, the transition and the evaluation model according to Equation 2 and 3 respectively. This recursive approach to the stochastic filtering enables sequential processing of the measurements, which is suitable for the real-time position estimation. The initial system state is determined at the time $k = 0$ with no available measurements $p(\mathbf{x}_0|\mathbf{z}_0) = p(\mathbf{x}_0)$.

Depending on the problem, it is required to define the transition and the evaluation functions, the state and the measurement noise, the system state and the measurement vectors. To ensure the real time computation, the number of parameters should be minimal, especially with the grid-based implementations as discussed in this thesis. In this case, the state is determined only by the 2D position:

$$\mathbf{x}_k = (x_k, y_k) \tag{6}$$

where x_k and y_k coordinates may be expressed as longitude and latitude. Nevertheless, in this implementation, the position is represented by integers with centimeter-level precision denoting a distance to the reference point in the map (as discussed in the

system description in Appendix A). When a step is detected, the posterior system state $\mathbf{x}_k$ is computed using recursive relations from the state at the time $k-1$. The current measurements vector at the time k is expressed as follows:

$$\mathbf{z}_k = (\theta_k, L, A_{map}) \tag{7}$$

where θ_k denotes the heading value in degrees and L is the detected step length. The value L is fixed in the evaluation and the influence of different values of the step length estimation are investigated. The parameter A_{map} represents the map model by storing information about the accessibility of positions in the building. Considering other positioning techniques, e.g., Wi-Fi fingerprinting or BLE, providing estimations independent to the previous estimations, they are suitable to be incorporated in the evaluation phase [52] instead of the transition which is only based on the PDR.

When a transition between floors is detected, the estimation model is reset ($k = 0$), a new map model is loaded and the current initial state is set according to the entry position.

Transition (Equation 2) is performed using the PDR relative position estimation (Equation 1):

$$\mathbf{f}_k(x_k, y_k) = (x_k + L \times \sin(\theta_k), y_k + L \times \cos(\theta_k)). \tag{8}$$

The state noise is a zero-mean white noise with the covariance matrix $cov(\mathbf{w}_k) = diag(\sigma^2, \sigma^2)$. Different standard deviation values σ were tested in author's referenced publications. Recommendations for the parameter configuration are discussed for all grid-based filters.

Evaluation (Equation 3) is based on the provided map model, as seen in this simplified function:

$$\mathbf{h}_k(x_k, y_k) = \begin{cases} 1 & \text{if } (x_k, y_k) \text{ is accessible} \\ 0 & \text{if } (x_k, y_k) \text{ is not accessible.} \end{cases} \tag{9}$$

Inaccessible positions in the building represent walls, restricted places, permanent obstacles and, in some cases, places outside the building or the map. However, determining the accessibility only from the location vector is not sufficient in most approaches. The direct PDR transition from an accessible point A to an accessible point B with a wall between them should be restricted. Related indoor localisation systems often incorporate the map model into the transition function. Fetzer et al. [27] investigate a navigation graph and a mesh approach where the transition is performed only along these structures preventing the step transition to intersect any obstacle. In this proposed approach, the transition is accomplished with no restrictions, but at the evaluation

stage, the accessibility is determined using both positions - the current one and the previous position, from which the transition was performed. Moreover, the main evaluation part depends only on the map model. Therefore in this implementation, the measurement noise is omitted, i.e., $\mathbf{v}_k = 0$.

3.2 Bayesian Filtering Implementations

Bayesian relations (defined in equations 4 and 5), applied on the PDR-based indoor localisation, specify only the conceptual solution of the filtering problem. Various implementations of the Bayes filters exist, from which the Kalman and the particle filter are the most frequent approaches applied on the indoor positioning problem. The belief distribution is approximated when certain assumptions for the exact solution calculation are not true, i.e., the analytic solution is intractable [90]. The optimal Kalman filter assumes the posterior density at every time to be Gaussian and the optimal grid-based filter requires the state space to be discrete with a finite number of states, that is not fulfilled in the indoor positioning problem. Three main approaches to approximate the density function are listed as follows:

3.2.1 Kalman Filter

The Kalman filter is a continuous filter, which parametrises the belief by a mean and a covariance:

$$p(\mathbf{x}_k|\mathbf{z}_{1:k}) \approx \mathcal{N}(\mathbf{x}_k, \mu_k, \Sigma_k) \tag{10}$$

where μ_k denotes the mean of Gaussian and Σ_k determines the $d \times d$ covariance matrix (where d is a number of state dimensions). To overcome the limitation of unimodal distributions, the multihypothesis tracking approach is defined as follows:

$$p(\mathbf{x}_k|\mathbf{z}_{1:k}) \approx \sum_{i=1}^{N_k} w_k^i \mathcal{N}(\mathbf{x}_k, \mu_k^i, \Sigma_k^i) \tag{11}$$

where N_k denotes the number of hypotheses (Gaussians) and w_k^i is a weight of the i-th hypothesis. If $\mathbf{f}_k$ and $\mathbf{h}_k$ (from equations 2 and 3 respectively) are not linear functions, extended Kalman filter (EKF) linearises the functions using the first term in a Taylor expansion. Alternatively, unscented Kalman filter (UKF) may be applied, since its deterministic sampling technique better approximates the nonlinearity. In general, the state computation using the Kalman filter or its derivatives has smaller computational demands compared to other approaches. However, if a probability density is non-Gaussian, the Kalman filter cannot describe it well.

3.2.2 Particle Filter

The particle filter is a stochastic Monte Carlo method which approximates a posterior distribution by a discrete set of samples called particles:

$$p(\mathbf{x}_k|\mathbf{z}_{1:k}) \approx \sum_{i=1}^{N_s} w_k^i \delta(\mathbf{x}_k - \mathbf{x}_k^i) \tag{12}$$

where w_k^i is a weight associated with the particle $\mathbf{x}_k^i$, N_s is a number of samples, $\delta(y)$ denotes a Dirac delta function for a point y and weights are normalized, i.e., $\sum_{i=1}^{N_s} w_k^i = 1$. The common implementation widely used for the indoor positioning is the sampling importance resampling filter (SIR), known also as the bootstrap filter [91] or the condensation particle filter [92]. One iteration of the filter consists of two basic steps - the sampling, according to the transition model, and the weight assignment, according to the evaluation model. These two steps form the sequential importance sampling (SIS) method. The SIR filter appends a resampling step to overcome a degeneracy problem causing all but one particle to have negligible weights. The resampling produces a new set of samples based on the existing set, where new particles are sampled from positions or states denoted by prior particles. Weights in the prior set of particles determine the sampling distribution. Typically, particle weights in the posterior set are assigned equally and the position estimation is based on the density of particles in a selected area. However, the resampling step may produce a loss of diversity (known as a sample impoverishment phenomenon). Other particle filtering methods may differ in this step which is performed not at every iteration, but only if a degeneracy measure is above a given threshold, e.g., the regularized particle filter resamples from a continuous approximation of the posterior density. The proposal distribution for sampling, called the importance density, influences the performance of the particle filter making the choice crucial in the entire process [90].

3.2.3 Grid-based Filter

The grid-based filter decomposes the state space into a grid structure, where the probability density value is associated with a single point, typically the center of the grid cell. Conceptually, the grid-based filter may be expressed in terms of points with associated weights or belief values like the particle filter. However, these points are not sampled at every iteration but predefined by the grid structure and unlike the particle filter, the computation is deterministic.

One of the biggest drawback of such approach is the computational cost growing exponentially with the increasing number of dimensions [87]. Therefore, only

low-dimensional state representations are suitable for the real-time indoor positioning systems. Another weakness of the method is the approximation precision, which is determined by the distance between two adjacent grid points. The grid covers the entire state space evenly. Therefore, the grid cannot focus on regions with the high probability density with a greater resolution. In this thesis, the grid design and the belief computation are discussed and the advanced point-mass (APM) filter is introduced, which overcomes the main drawbacks of the grid-based approach. This method enables to focus only on regions with relevant probability density values using one or more scalable and rotatable grids.

3.3 Related Applications of Bayes Filters

Various implementations are present also in systems using different devices than the smartphone, e.g., the unscented Kalman filter [93] for the robot localisation or the particle filter for chest-mounted IMU [94]. The grid-based approach is most common in robot positioning. Burgard et al. [95] modeled the system state with a three-dimensional grid consisting of the position and the direction with the resolution 15 cm $\times$ 15 cm $\times$ 1 degree. Herrero-Peréz et al. [96] introduced fuzzy positioning grids to reduce computational complexity. The three-dimensional grid is used for the robot localisation where the system state is defined by the 2D position and the direction. One of a few grid-based solutions for pedestrians is proposed by Xu et al. [97].

Most frequent implementations for the indoor positioning are Kalman and particle filters. Hafner et al. [98] compared these two filters resulting to the better performance of the particle filter either on the imperfect trajectory obtained using Wi-Fi or with fewer available access points. Related publications propose various approaches to the indoor positioning including the sensor fusion mostly based on PDR and Wi-Fi. Fetzer et al. [27] elaborated the particle filter, where the state of each particle is described by the three-dimensional position and the direction. The evaluation stage is based also on the Wi-Fi data and the activity recognition output. Chen et al. [75] fused Wi-Fi and PDR using Kalman filtering technique in order to keep the low computation demands. Furthermore, landmarks (e.g., turns, elevators, stairs) are incorporated into the proposed system. Villien et al. [16] adapted the particle filter for the sensor fusion. Only the subset of particles is resampled at each time step. Moreover, the computation is performed not only after detected step but also with a sufficient number of RSS measurements with high values. Radu and Marina [65] introduced a system, where particles are updating their weights based on the Wi-Fi, orientation, distance, and output from the activity recognition method. Moreover, Ning and Chen [99] incorporated the

magnetic fingerprint map to the particle filter evaluation stage. Xu et al. [42] enriched the system based on the particle filter with the light sensor measurements to utilize luminaries in the indoor space. Bojja et al. [74] combined the dead reckoning method with the 3D map matching on the user localisation in a parking garage and introduced a method to distinguish between the pedestrian and the vehicle positioning.

The particle filter is a popular method for the sensor fusion and for the error reducement gained by the PDR approach. Practical tips for the adaptation of the method on indoor positioning are present in some publications. The position estimation is selected from the posterior system state, i.e., the list of weighted particles. In case of multimodal distribution, the position is unlikely between these modes as often calculated and the suggestion is to choose a mode for the location [27]. Landa et al. [100] modified the particle filter to use mutable number of particles according to the level of convergence and allows an initialization of a few new particles at each iteration to ensure the system does not converge to the wrong location. In bachelor thesis [10], supervised by author of this dissertation, the particle filter and the parameter configuration were investigated. Promising results were obtained when the particles contains the step length estimation value in their state.

The particle filter implementation by Teammco and Xie [101] was chosen as the reference method for the comparison with the grid-based filters introduced in this thesis. The particle filter uses the location and the direction as the system state. They rotate particles according to the turn obtained from sensors. However, experiments based on our implementation [3] suggests that better results are obtained when the absolute direction is considered in this computation. Furthermore, the version with only 2D position may be more relevant for the comparison with proposed methods. The particle filter is a stochastic method, i.e., the output trajectory is different when the run is repeated with the same configuration. Our evaluation produced the relative variation under 5% on the experiments which achieved sufficient errors. In general, the method is suitable for the real time indoor positioning as it is easily scalable by defining the number of particles included in the computation.

4 Grid-Based Bayes Filters

The thesis is focused on grid-based implementations of the Bayes filtering. In this chapter, grid-based methods published in [2], [3], and [4] are introduced. Some features extending the core filtering are omitted, e.g., auto-correction methods [2]. The discussion about the parameter configuration is summarized with the recommended settings for selected filters. Moreover, comments on the sensor fusion are presented.

4.1 Grid Filter and Grid Design

The grid filter is a deterministic implementation. When applied on the indoor positioning, it covers the full area of the map but is not able to focus on the selected area where the relevant position is estimated with more detail as the particle filter does.

The map in a form of a floor plan is tessellated into a regular grid consisting of N_s grid cells $\{\mathbf{x}_k^i : i = 1, \ldots, N_s\}$ or N_s isolated points $\{\bar{\mathbf{x}}_k^i : i = 1, \ldots, N_s\}$. Typically, $\bar{\mathbf{x}}_k^i$ is a center of the grid cell $\mathbf{x}_k^i$. In the basic version of the grid filter, the value N_s and positions of points are immutable at every time k. The probability distribution is approximated at these points with associated weights w_k^i, likewise the particle filter:

$$p(\mathbf{x}_k|\mathbf{z}_{1:k}) \approx \sum_{i=1}^{N_s} w_k^i \delta(\mathbf{x}_k - \mathbf{x}_k^i). \tag{13}$$

In this case, the weight or the belief value of a point denotes the probability that the current position is within the grid cell. The probability density after the prediction stage execution is expressed as

$$p(\mathbf{x}_k|\mathbf{z}_{1:k-1}) \approx \sum_{i=1}^{N_s} \bar{w}_k^i \delta(\mathbf{x}_k - \mathbf{x}_k^i) \tag{14}$$

where weights $\bar{w}_k^i$ are computed from the prior grid using the transition model:

$$\bar{w}_k^i \approx \sum_{j=1}^{N_s} w_{k-1}^j p(\bar{\mathbf{x}}_k^i|\bar{\mathbf{x}}_{k-1}^j). \tag{15}$$

Weights in the posterior state are computed using the predicted weights $\bar{w}_k^i$ and the evaluation model followed by the normalization

$$w_k^i \approx \frac{\bar{w}_k^i p(\mathbf{z}_k|\bar{\mathbf{x}}_k^i)}{\sum_{j=1}^{N_s} \bar{w}_k^j p(\mathbf{z}_k|\bar{\mathbf{x}}_k^j)}. \tag{16}$$

In Equation (15), the belief value is calculated using a convolution. Convolution masks depend on transition and noise models and define how the probabilities are redistributed during the prediction stage. Moreover, masks may be precomputed to reduce the computation time of a single iteration. In our implementation, masks are stored for every considered step length and for 360 distinct directions. Convolution masks are significantly smaller than the entire grid since the transition probability $p(\bar{\mathbf{x}}_k^i|\bar{\mathbf{x}}_{k-1}^j) = 0$ for all pairs of points with the distance greater than a single step length plus the maximal noise value.

Even though Equation (15) describes a single step in the process where the weights are calculated in a loop iterating over posterior grid cells, our implementation iterates over grid cells in the prior grid. This approach allows to perform the computation only for grid cells with non-negligible belief values. The evaluation is merged with the transition during the convolution. Therefore, it is possible to include the verification of the transition, i.e., the accessibility of a grid cell is determined not only by its position but also by the verification whether the transition is possible. A path between such two grid cells is constructed using a line drawing algorithm. A transition is possible if all grid cells on the path are accessible (e.g., corresponding to a wall). These paths are precomputed for all pairs of grid cells in the mask.

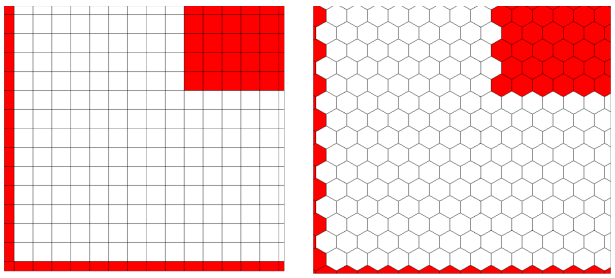

Fig. 2: A part of a floor plan tessellated into a grid consisting of squares or hexagons. The distance between all adjacent cells is the same in all six directions in the hexagonal grid.

A single iteration of the grid filter is performed when a step is detected. Initially, the mask is loaded and applied using the convolution. The posterior grid is normalized (Equation 16) and the position estimation is selected as the point $\bar{\mathbf{x}}_k^i$ with the maximum belief value w_k^i. Different grid designs were elaborated. The drawback of the grid filter with square grid cells is that the distance between two adjacent cell centers is not the

same in all direction which is fulfilled in the hexagonal grid (Figure 2). The influence of the grid design is investigated and the square grid is used for improved methods of the filter. For the purpose of the evaluation, the latter is called the hexagonal grid filter. Two versions of square-shaped grid filter are considered depending on the convolution mask computation as discussed later.

4.2 Convolution Masks and Fine Mask Grid Filter

The convolution is an essential part of the grid-based filters enabling to finish the computation before the next step is detected. Grid cells with positive belief values in the prior grid are iterated in order to calculate the posterior grid belief values. A weight in the posterior grid at the time k is computed as follows:

$$w_k^t = w_k^t + m_{\alpha,L}^{t-i} w_{k-1}^i \mathbf{h}(i,t) \tag{17}$$

where the index i corresponds to the prior grid $i = \{b \in \{1,\ldots,N_s\} : w_{k-1}^b > 0\}$. In case of a very large N_s, it is possible to limit the number of active cells by setting the threshold for negligible weights. i.e., to use the selected threshold T for indices $i = \{b \in \{1,\ldots,N_s\} : w_{k-1}^b > T\}$. The index t denotes the grid cell in the posterior grid. The function $\mathbf{h}(i,t)$ extends the evaluation phase of the filtering based on the map model with the verification of the transition, i.e., not only the accessibility of the cell at index t is inspected but the whole path between these two cells. The current system consider only values one for allowed transition and zero otherwise with the possibility to utilize more values with an advanced map model.

Convolution masks model the transition including the transition noise. The mask for a given direction α and a step length L is expressed as $M_{\alpha,L} = \{m_{\alpha,L}^j : j = -N_m,\ldots,0,\ldots,N_m\}$, where the position with the index 0 determines the origin, i.e., the mask position associated with the grid position where the mask is applied. The mask size $2N_m + 1$ is selected to cover relative relevant positions of grid cells which are affected by the convolution. Typically, the required size of the mask is derived from the grid cell size, the step length distribution (three-sigma rule) and the noise. The value $m_{\alpha,L}^j$ represents the probability of the transition from the origin position ($j = 0$) to the relative position at the index j. The value $m_{\alpha,L}^0$ encodes the probability of no movement.

The inaccuracy of the estimated step length and the measured direction is incorporated using normal distributions with the mean at the expected values. The choice of standard derivation values is defined as one of our research questions. Two techniques are applied to construct the convolution mask. The first method calculates the

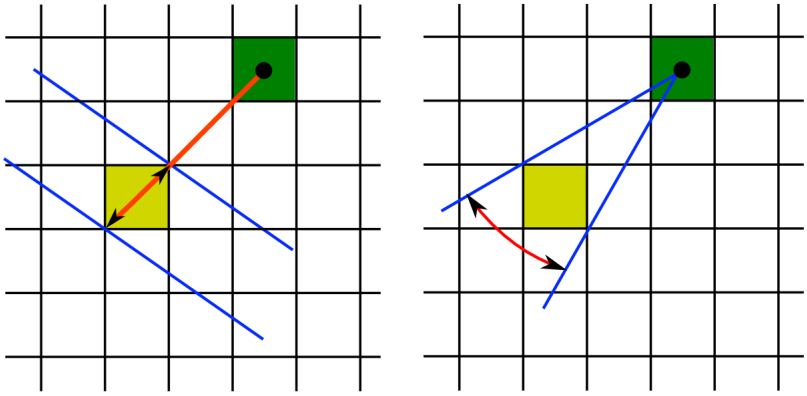

Fig. 3: The calculation of the convolution mask based on normal distributions of the step length and direction. The green cell denotes the origin of the mask and the yellow cell weight is computed.

weight of a single grid cell as a product of step length and direction probabilities determined by the cumulative distribution functions regarding the bounds of the grid cell as demonstrated in Figure 3. Another approach of the mask construction is to use an additional layer of points with the smaller distance between adjacent points. The probability density is calculated for all points according to their distance and direction from the origin of the mask. The grid cell weight is expressed as a sum of all values within the cell. Weights in the mask are normalized.

The basic grid filter and the hexagonal grid filter are based on the first approach. The fine mask grid filter has the same implementation as the basic grid filter with the only difference in the convolution masks construction.

4.3 Centroid Grid Filter

One of drawbacks of the grid-based filters is the fixed resolution. Unlike the particle filter, which is capable of producing particles in the area of the expected position, the grid design is determined in advance. The size of the grid cell is limited by the total area of the building to cover. The introduced centroid grid filter reduces the impact of the space discretisation. The same amount of grid cells is used but an additional grid is incorporated for the point position calculation, i.e., the estimated position is not defined as the center of the grid cell but as a point in the fine grid layer (Figure 4).

The coarse grid G_k (identical to the grid in previous methods) consists of N_s grid cells $G_k = \{\mathbf{x}_k^i : i = 1, \ldots, N_s\}$. Every grid cell $\mathbf{x}_k^i$ is associated with the weight value w_k^i (Equation (13)), the position estimation expressed as $\bar{\mathbf{x}}_k^i$, and a fine grid of N_u points $G'_{k,i} = \{\mathbf{x'}_k^{ij} : j = 1, \ldots, N_u\}$. In this approach, the $\bar{\mathbf{x}}_k^i$ is not the center of the grid cell,

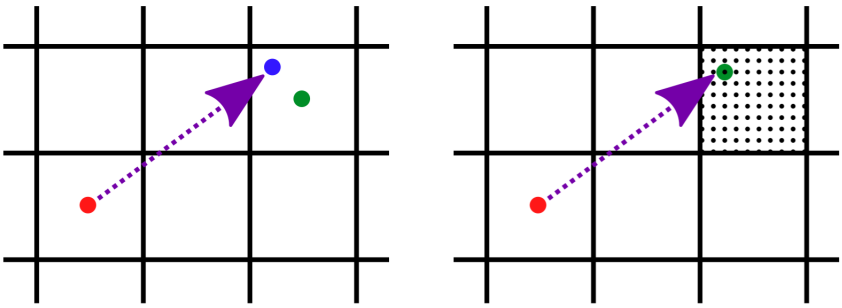

Fig. 4: The arrow denotes the transition from the red point. In the left figure, the transition ends in the blue point. However, previous methods sets the estimated position in the green point for the next iteration. In the right figure, the centroid grid filter selects the centroid of the corresponding grid cell.

but selected from the set of points $G'_{k,i}$. A so-called centroid of a coarse grid cell $\mathbf{x}_k^i$ is labeled as c_k^i, and it denotes the corresponding index in the $G'_{k,i}$, i.e., $c_k^i = j$ such that $\bar{\mathbf{x}}_k^i = \mathbf{x}'^{ij}_k$. The fine grid covering the entire state space is defined as $G'_k = \bigcup_{i=1}^{N_s} G'_{k,i}$. Positions of points in both layers of grids are immutable. When a step is detected, the weights are calculated according to the convolution mask. Moreover, centroids for all coarse grid cells are selected. The belief values in the posterior grid are derived from the prior grid using the formula

$$w_k^t = \sum_{i=1}^{N_s} w_{k-1}^i m'^{i-t}_{\alpha,L,c_{k-1}^i} \mathbf{h}(i,t) \qquad t = 1, \ldots, N_s \tag{18}$$

where the function $\mathbf{h}(i,t)$ is zero for the invalid transition from the grid cell at index i to the position at the target index t and one otherwise. The value $m'^{i-t}_{\alpha,L,c_{k-1}^i}$ is obtained from the mask $M'_{\alpha,L,c} = \{m'^{j}_{\alpha,L,c} : j = -N_m, \ldots, 0, \ldots, N_m\}$. The mask is constructed as for the fine mask grid filter with the extension that the value $m^{i-t}_{\alpha,L,c}$ denotes the probability of the transition from the centroid position at index i to the origin, i.e., the target grid cell where the weight is computed. The so-called centroid is selected for all coarse grid cells from the set of corresponding points in the fine grid layer:

$$c_k^t = \frac{\sum_{i=1}^{N_s} w_k^{i\to t} c_k^{i\to t}}{w_k^t} \qquad t = 1, \ldots, N_s \tag{19}$$

where $w_k^{i\to t} = w_{k-1}^i m'^{i-t}_{\alpha,L,c_{k-1}^i} \mathbf{h}(i,t)$ is the summand expressed in Equation (18), i.e., $w_k^t = \sum_{i=1}^{N_s} w_k^{i\to t}$. The value $c_k^{i\to t}$ is precomputed and stored with the mask values determining the most relevant target fine grid index, when the probability is transformed from a coarse grid cell i to the cell t.

Masks in previous approaches are designed as distributing masks, i.e., the value in the mask defines the probability of the transition from the origin to the given target

point. During the convolution process, prior grid cells are iterated and the mask determines how the current belief value is distributed in the posterior grid. However, the centroid grid filter uses the reversed approach. The mask value defines the probability of the transition from the given point to the origin. Moreover, centroids are computed for all posterior grid cells with positive belief values.

Masks are precomputed for all combinations of step lengths L, step headings α and centroid indices c. In the implementation, it is beneficial to store the list of active prior grid cells (with nonnegligible values). The weight calculation (Equation (18)) is not performed for all coarse grid cells. Active prior grid cells are iterated to label the target grid cells (within the selected area according to the mask). The convolution is performed continuously for all obtained target grid cells. The centroid computation extends the process of the posterior state calculation. Therefore, less grid cells may be processed in real time compared to other methods. If the reduction of active grid cells is required, these values (lower than a selected threshold) may be set to zero in the correction phase before the normalization. Another approach which produces more stable results but with some additional computation, sorts the belief values and confirms only a fixed number of values. The risk of such methods is that in some scenarios (inaccurate parameter configurations and zero probability of false step detection) the knowledge of the position may be lost.

4.4 Advanced Point-Mass Filter

The advanced point-mass filter (APM) combines strengths of the grid-based filters and the particle filter. Using all benefits of the grid approach, the APM computes belief values on a predefined grid using the convolution deterministically. Moreover, the computational complexity, as the main drawback of grid-based solutions, is reduced by using adapting grids which are rotated and placed on the relevant area with a desired resolution. Therefore, the impact of the discrete approximation of probability density function is decreased. Unlike other grid approaches, the dynamic grid design allows to avoid resetting belief values if the number of active points exceeds the limit, which prevents the filter from the loss of estimation. The method introduced by Šimandl et al. [102] is elaborated with the adaptation on the indoor positioning problem. In the referenced work, no loss of accuracy is achieved with lower computational demands compared to the particle filter on the nonlinear state estimation problem.

A probability distribution at the time k is represented by a grid of N_k points $G_k = \{\mathbf{x}_k^i : \mathbf{x}_k^i \in \mathbb{R}^2, i = 1, \ldots, N_k\}$, by a set of volume masses for grid cells $\mathcal{D}_k = \{\Delta\mathbf{x}_k^i, i = 1, \ldots, N_k\}$, and a set of belief values at the grid points $\mathcal{P}_k = \mathcal{P}_{k|1:k} = \{w_k^i :$

$w_k^i = p(\mathbf{x}_k^i|\mathbf{z}_k), \mathbf{x}_k^i \in G_k\}$. A set of belief values, after the convolution is performed, is defined as $\bar{\mathcal{P}}_k = \mathcal{P}_{k|1:k-1} = \{\bar{w}_k^i : \bar{w}_k^i = p(\mathbf{x}_k^i|\mathbf{z}_{k-1}), \mathbf{x}_k^i \in G_k\}$. The volume mass of a grid cell is for the introduced two-dimensional positioning problem interpreted as the area covered by the grid cell. The APM filter assumes points to be centers of the corresponding grid cells. The main scheme of the algorithm is defined as follows:

Initialization: Define an initial state represented by a grid G_0, D_0, and P_0 for the prior PDF $p(\mathbf{x}_0)$. Then, proceed to following four steps for $k = 1, 2, 3 \ldots$.

(1) Filtering: Compute values of the approximate filtering pdf at points of the grid G_k using Equation (5) for the correction stage, for $i = 1, \ldots, N_k$:

$$w_k^i = c_k^{-1} \bar{w}_k^i p_{\mathbf{v}_k}(\mathbf{z}_k - \mathbf{h}_k(\mathbf{x}_k^i)) \tag{20}$$

where $p_{\mathbf{v}_k}(\mathbf{z}_k - \mathbf{h}_k(\mathbf{x}_k^i))$ denotes the evaluation $p(\mathbf{z}_k|\mathbf{x}_k)$ from Equation (5) and the normalization constant is defined as $c_k^{-1} = \sum_{i=1}^{N_k} \Delta\mathbf{x}_k^i \bar{w}_k^i p_{\mathbf{v}_k}(\mathbf{z}_k - \mathbf{h}_k(\mathbf{x}_k^i))$. As the measurements depend only on the map model, its integration is included in the algorithm during the convolution phase likewise the grid-based filter implementation. Therefore, the filtering step consists only of the normalization

$$w_k^i = \frac{\bar{w}_k^i}{\sum_{i=1}^{N_k} \Delta\mathbf{x}_k^i \bar{w}_k^i}. \tag{21}$$

Optionally, the negligible belief values may be reset to zeros. In this step, the grids are split, if necessary in the multigrid version of the filter and the weights of the grids are computed.

(2) Time Update of Grid: Transform the grid G_k to a grid $H_{k+1} = \{\mathbf{y}_{k+1}^i : i = 1, \ldots, N_k\}$ with the equal number of points using the PDR system dynamics:

$$\mathbf{y}_{k+1}^i = \mathbf{f}_k(\mathbf{x}_k^i) \qquad i = 1, \ldots, N_k \tag{22}$$

where $\mathbf{f}_k$ denotes the state transition function defined in (8). In general, the transition function is allowed to be nonlinear and the grid H_{k+1} may have different structural properties than G_k. The grid H_{k+1} integrates the state transition noise and covers the support of PDF, i.e., the relevant area, where positive belief values would occur. The local predictive mean and the covariance matrix is calculated and the grid merging for multigrid APM is executed, if necessary.

(3) Grid redefinition: Redefine the grid H_{k+1} to obtain a new grid $G_{k+1} = \{\mathbf{x}_{k+1}^i : i = 1, \ldots, N_{k+1}\}$ for the state $\mathbf{x}_{t+1}$, incorporating the state noise $\mathbf{w}_t$, with the same structural properties as the original grid G_k. The number of points N_{k+1} may be different than the value N_k in the preceding state. Compute the number of points, $\mathcal{D}_{k+1}$, and rotate the grid according to a computed transformation matrix.

(4) Prediction: Compute values of the approximate predictive PDF at the new grid G_{k+1} using (4) for $i = 1, \ldots, N_{k+1}$:

$$\bar{w}_{k+1}^{i} = \sum_{j=1}^{N_k} \Delta \mathbf{x}_k^j w_k^j p_{\mathbf{w}_k}(\mathbf{x}_{k+1}^i - \mathbf{y}_{k+1}^j) \tag{23}$$

where $p_{\mathbf{w}_k}(\mathbf{x}_{k+1}^i - \mathbf{y}_{k+1}^j)$ denotes the transition PDF $p(\mathbf{x}_{k+1}|\mathbf{x}_k)$, $\mathbf{x}_{k+1}^i \in G_{k+1}$ and $\mathbf{y}_{k+1}^i \in H_{k+1}$. Predictive belief values are calculated using the convolution from corrected belief values $\mathcal{P}_k$ and grid points determined by the grid H_{k+1}.

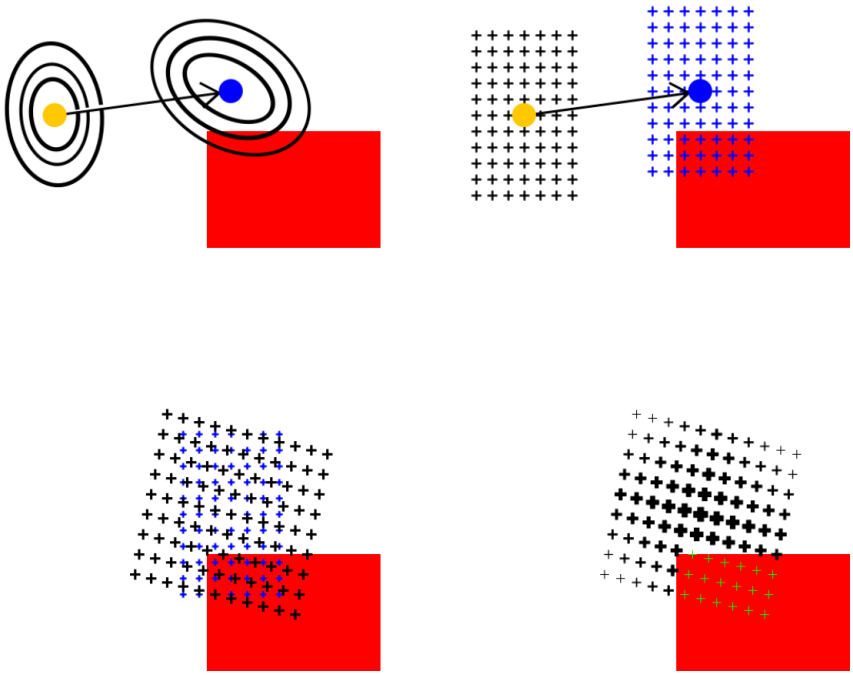

Fig. 5: A single iteration of APM consists of the transition according to the PDR (from the yellow point to the blue point), which is modeled by grids. A new redefined grid may be rotated and with different number of points. The convolution computes the belief values with respect to the walls and obstacles.

Figure 5 demonstrates the process of the transition according to the PDR, the grid redefinition and the convolution. Unlike other grid-based filters, the transition is not included in the convolution. The transition of all grid points is performed in the time update phase. The convolution models the noise, i.e., the normal distribution have the mean zero instead of the estimated step length.

The essential part of the APM method is extended with features for the efficient application. Authors of the method introduced the multigrid version of the filter and

the grid design calculation. Only a single grid is not sufficient in complex indoor environments since the probability distribution may be multimodal. This phenomenon is tractable using the particle filter, the grid-based filters and also with multihypothesis versions of the Kalman filter. In the multigrid APM, weights are assigned to all grids. Moreover, split and merge operations are performed. Grids are split during the filtering phase if there are separable areas considering the marginal densities for all dimensions. Even though it is recommended to perform this process repeatedly, our experiments suggest that the single iteration of the split is sufficient. The grids are merged after the transition using the Mahalanobis distance between a point and a distribution. These methods are a trade-off between the optimal solution and the computational demands.

The thrifty convolution is similar to the approach applied for other grid methods. Only significant points in posterior grids are derived for the computation based on the distance from the considered source point in the prior grid. Even though, the masks cannot be precomputed, it is possible to reduce the time of the convolution by caching these values. Moreover, the grid design in terms of the number of points and their distances is introduced by the authors of this approach. However, the upper bound of the maximum number of points in a single grid was introduced in our experiments to satisfy the requirement of real-time computation.

4.5 Parameters Configuration and Sensor Fusion

Various parameters influence the overall success of selected Bayesian filtering methods. One of the essential components is the step length estimation. Despite the existence of approaches for the step length calculation, our evaluation is based on the fixed estimation. The evaluation investigates the capability of filters to deal with underestimated and overestimated step lengths.

The noise is modeled using the normal distribution. After the transition, the target grid cell according to the PDR does not gain the belief value from the source cell in the prior grid, but this probability is distributed to other cells within a selected range, even though the target cell receives the maximum gain. Grid-based methods (the basic GF, the hexagonal GF, the fine mask GF, and the centroid GF) perform this process in the convolution using the normal distribution of the step length and the direction. Figure 6 portraits the area where values, obtained from the distribution, are within one-sigma. Standard deviations for the step length normal distribution (step SD) and for the direction distribution (turn SD) are required to be selected. Experiments [3] suggest to use the value 15 cm for the robust positioning. Smaller values may be beneficial with increasing confidence in the configuration accuracy (i.e., with improved step length

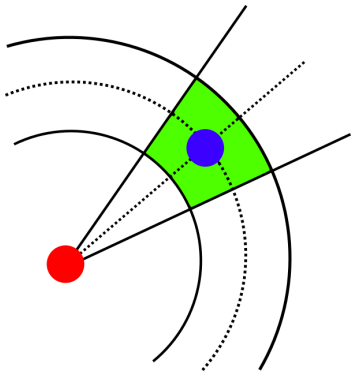

Fig. 6: The red point denotes the source position and the blue point the target location according to the PDR. Dotted lines represents the mean of the step length and the direction normal distributions. The green area is within one-sigma.

estimation). However, the position may be lost with smaller values. It is caused by the convolution mask implementation if there is zero probability of false step detection, i.e., the weight of the origin grid cell in the mask is zero. When the knowledge of the position is lost, the recovery method should be applied. One of the possibilities is to recall the previous estimation as an initial value or to utilize other components (e.g., Wi-Fi) for the current estimation. Similar approach is recommended for the turn SD, i.e., the value up to 30 cm with the smaller values if the step length is known.

The grid size used for all grid-based filters is 33 $\times$ 33 cm. Considering fine grid layer, the grid size is 3 $\times$ 3 cm. Therefore, the convolution mask for the fine mask grid filter is calculated as a sum of 121 points, i.e., 11 $\times$ 11 points with the distance 3 cm between two adjacent points.

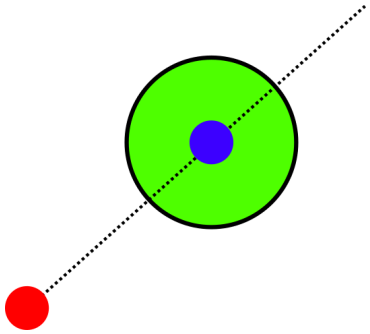

Fig. 7: The transition is performed from the red point to the blue point according to the PDR. The green circle denotes the one-sigma area of the normal distribution for the noise.

The APM separates the transition and the convolution. Only the normal distribution for the distance is considered in this case. Figure 7 demonstrates the area of

values within one-sigma from the distribution. This approach is applied also for particle displacement in the particle filter with only 2D position as the system state used in the evaluation. Best results in the evaluation are obtained using the standard deviation greater than 20 cm.

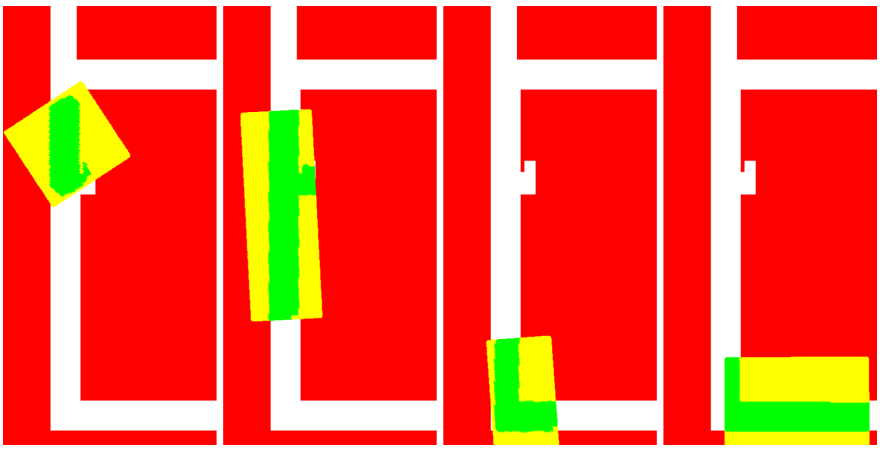

Fig. 8: The APM with a single grid able to scale and rotate according to the certainty of the position estimation. Green points gain positive weight values, yellow points have zero belief since they are placed in the red inaccessible area.

Figure 8 demonstrates the ability of a grid in the APM to cover the relevant area by rotating and scaling. Multiple parameters are available to configure the APM. The value γ influences the number of points in the grid. It was required in our evaluation to limit the maximum number of points in a single grid. Another parameter K defines the threshold for the merging two grids based on their mahalanobis distance. Observations suggests to increase the value K to achieve less grid split and merge events and hence to reduce the time of the computation.

In our implementation, the evaluation stage of the Bayesian filtering consists only of the map model integration. In grid filters, it is incorporated into the convolution. Using other sources of information, e.g., Wi-Fi fingerprinting, the evaluation stage of the filters is extended with the correction of the current state according to the measurements. The probability value for every grid cell covering the map is computed and a belief value for a specific grid cell is calculated as a product of the recent value and the probability based on the measurement map. The state is normalized as a part of the Bayesian filtering iteration. In general, all points with assigned belief values are updated according to the current measurements. These points are on fixed positions in grid-based filters (these positions vary in the centroid grid filter) or are placed freely on the map (particle filter, APM). Measurement values should be calculated for all these positions. If necessary, the discretisation may be introduced. As an example, a

small value measured by the light sensor suggests that the current position is inside the building. The probability for all positions within the building is high and the value for positions outdoors is low. In more advanced model, these values may vary according to the situation (e.g., lobby with more windows compared to corridors). The current state is updated according to the light probabilities. Belief values for all positions outside the building are reduced.

Another approach to the fusion with other methods is to use them as landmarks. When a floor transition, an indoor-outdoor transition, or another type of activity or context is detected with the known position, the filter is restarted with the new initial position. In case of not exact location knowledge, the initial belief distribution is set according to the situation, e.g., positive probability values are set near elevator doors when the floor transition using elevators is recognized.

5 Evaluation

Introduced methods are evaluated in three different buildings, parameter configurations are investigated, and the output results of grid methods are compared with the particle filter. The system was evaluated using the recommended black-box approach [13] and particular methods were not examined separately. Observations suggests that some of them are reliable, e.g., the floor transition detection based on barometer measurements. The F1 score 97.1% was obtained for the step detection [2]. During longer sequences of steps the accuracy is increased. Nevertheless, the system is able to recover from a misdetected step or a false step as this occurs only as a single event not consecutive for multiple steps. Moreover, datasets for the precise evaluation of some methods, e.g., the step length estimation, are difficult to obtain.

All experiments were performed in the same manner. A subject with handheld smartphone walks along the predefined path. All raw sensor measurements are stored. Several checkpoints with known ground truth positions are placed along the path and indicated in data manually by the user pressing the button in the application when crossing the label on the floor. The Euclidean distance between the estimation and the ground truth position is calculated for all checkpoints. The main criterion is the third quartile of the error on all checkpoints to compare considered methods and configurations. Moreover, the penalty may be added for the floor misdetection which is not the case in this evaluation.

More than 3 000 simulations were performed using given sensor measurements. Observations of the parameter configurations and results are discussed. The core sensor measurement recordings, map models, output trajectories, and visualisations are available [103]. The evaluation explores techniques to achieve the best result with the current system configuration and also with regard to the reliability. However, better results may be achieved using other approaches, e.g., step length calculation, Wi-Fi or BLE integration.

5.1 Methods and Evaluation Goals

Six different versions of Bayes filters were implemented and evaluated:

1. **Basic Grid Filter** using square-shaped two-dimensional grid as introduced in Section 4.1 with convolution masks calculation based on the grid cell bounds (Section 4.2).

2. **Hexagonal Grid Filter** utilizes the same approach as the basic GF but grid cells are hexagonal-shaped (Section 4.1).

3. **Fine Mask Grid Filter** differs from the basic GF in the mask design. The two layer method of the mask construction proposed in Section 4.2 is applied.

4. **Centroid Grid Filter** utilizes the square-shaped grid where the position is not attached to the center of the grid cell but is selected from a set of points on the fine grid (Section 4.3).

5. **Advanced Point-Mass Filter** (APM), proposed by Šimandl et al. [102], is adapted and applied on the indoor localisation according to Section 4.4.

6. **Particle Filter** (PF) is selected for the comparison with grid-based filters. The SIR particle filter implementation introduced by Teammco and Xie [101] is applied. However, the state of particles does not include the direction.

Three venues with different conditions are taken for the evaluation. A faculty building in Slovakia with a simple custom path designed for the overall observations, especially when turning on the corner of two corridors. The device, subjects, and other details are known and the path is short compared to other venues making it suitable for rapid evaluation of selected approaches. Research questions for this scenario are:

- What is the general performance of selected methods? Are they suitable for the indoor positioning?

- How do grid-based methods deal with the underestimated and overestimated step length estimations?

- What is the stability of proposed methods, e.g., when the floor plan is rotated for the map model construction?

Another scenario is a shopping mall in France. The IPIN 2018 competition includes the on-site track along a challenging path with visitors and a dataset for the evaluation. The questions are as follows:

- What is the accuracy of the introduced system in a real scenario?
- Are observations based on a simple path in the faculty building applicable on the larger scale?
- What are the most suitable parameter configurations for all methods? Which method is the most reliable for the deployment?
- Is the floor transition detection producing satisfactory results?
- What is the best possible accuracy for all considered filters on the most comprehensive path?
- Do grid filters achieve better results compared to the respective implementation of the particle filter?

IPIN 2019 competition in a research institute in Italy provides a dataset for the evaluation. Moreover, results and observations from the on-site and off-site tracks are discussed. The research questions are as follows:

- How robust is the proposed system? Is it ready for the application on a different type of building?
- Does the configuration based on the dataset from the shopping mall achieve satisfactory results?
- What is the accuracy of proposed methods? What is the level of accuracy in the off-site track with the same system as for the on-site track but with the possibility of various configurations application?

5.2 Faculty Building - General Observations

The custom 85 m long path (Figure 9) was set in the faculty building (Park Angelinum 9, 04001 Košice, Slovakia). Seven runs were performed with six subjects. Their expected step lengths $\{79.1, 91.1, 79.1, 84.7, 66.4, 78.0\}$ were measured as the average length considering the covered distance after 20 performed steps. The experiment was supported with the video recording which was synchronised with sensor measurements. The output was visualized and analyzed to observe tendencies using various methods and configurations.

The main observation is that the building structure improves the accuracy of the positioning method. Table 1 contains errors on all checkpoints for different step

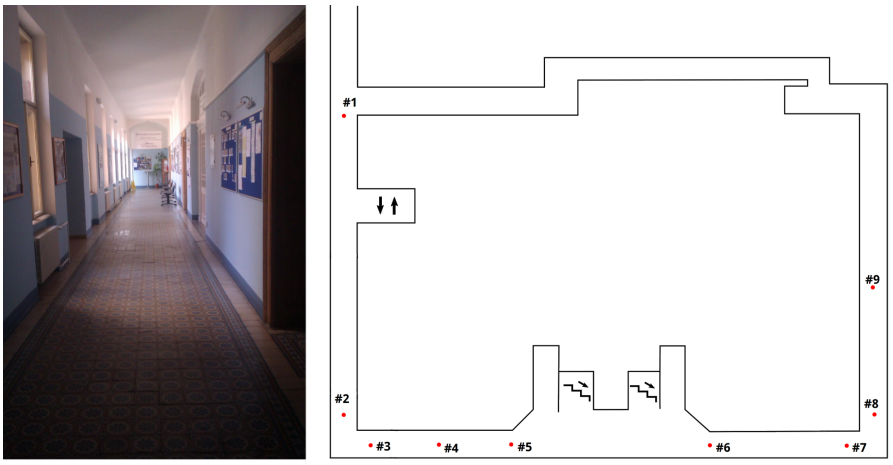

Fig. 9: The faculty building in Slovakia with a single floor path consisting of nine checkpoints.

lengths. Markers #3 and #8 are placed after the turning maneuver where the direction changes by 90° after a few consecutive steps. Typical situations for underestimated and overestimated step lengths are portrayed in Figure 10. The incorrect step length estimation may be detected when a distance between two consecutive steps is impossible to perform with a single step. However, a few steps are needed for full recovery of the current position (#8 and #9 for 70 cm in Table 1) Considering the overestimated step length, a few positions may be detected in the same area, i.e., the distance between these positions is significantly smaller than the step length or even zero. In this case, the system is able to recover as well (#8 for 90 cm in Table 1). The ability to recall the true trajectory is influenced by the method configuration and the building structure. Figure 11 demonstrates the path for the 60 cm step length where the true path was correctly detected after the first turn but the misdetection occurs after the longer straight walk.

Table 1: Position errors on 9 checkpoints in meters for the same trial with different configurations. The measured step length of the subject was 78 cm.

Step L.	#1	#2	#3	#4	#5	#6	#7	#8	#9	75% perc.
60 cm	0.7	5.9	6.7	2.7	3.9	7.8	10.1	10.9	16.9	10.12 m
70 cm	0.7	3.0	1.6	1.4	1.9	4.2	5.5	5.4	1.7	4.17 m
80 cm	0.7	0.5	0.3	0.1	0.2	0.5	1.0	0.5	0.4	0.53 m
90 cm	1.0	3.0	0.8	1.3	1.8	3.1	3.8	1.4	1.7	3.04 m

The performance of grid-based approaches was analyzed. Figure 12 displays the cumulative distribution functions for selected methods. Errors on all checkpoints (2 556 positions) with various step lengths (70, 80, 90) and standard deviations (5, 15) are grouped by the grid filter approach excluding trials with the loss of position. Consi-

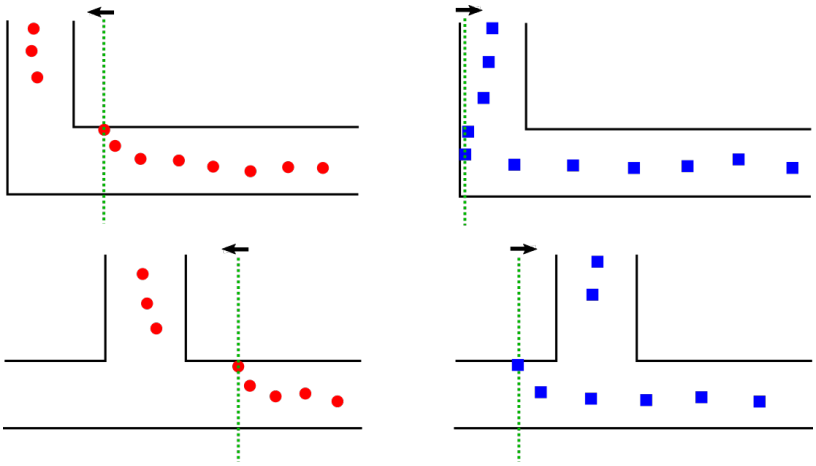

Fig. 10: Position estimations around junctions with underestimated step lengths (red points) and overestimated step lengths (blue points). Steps are taken from the right to the left and upper part of the figure.

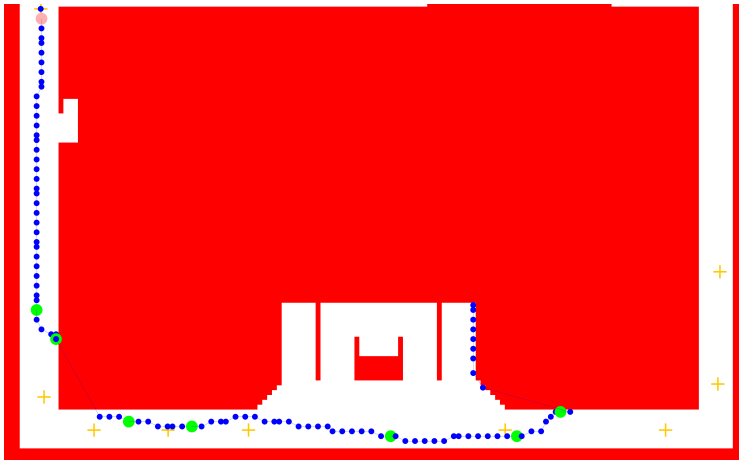

Fig. 11: The path of position estimations with the underestimated step length 60 cm. The expected step length of the subject is 78 cm.

dering various configurations, the two layer approach for grid or mask computation outperformed the basic and hexagonal grid filters.

The faculty building and also lots of other types of buildings consist of regular corridors mostly parallel or perpendicular to each other. The typical orientation in the map model is west-east or north-south for these corridors. An experiment was performed where the map was rotated by 45°. Out of 28 configurations, the difference on the same checkpoint was 19× under 1 m and 25× under 2 meters. Despite some larger errors with inaccurate step length estimations, no significant differences in errors were observed in general. The APM and the particle filter are map rotation independent methods. However, the grid tessellation is applied for the final position estimation leading to possible minor differences.

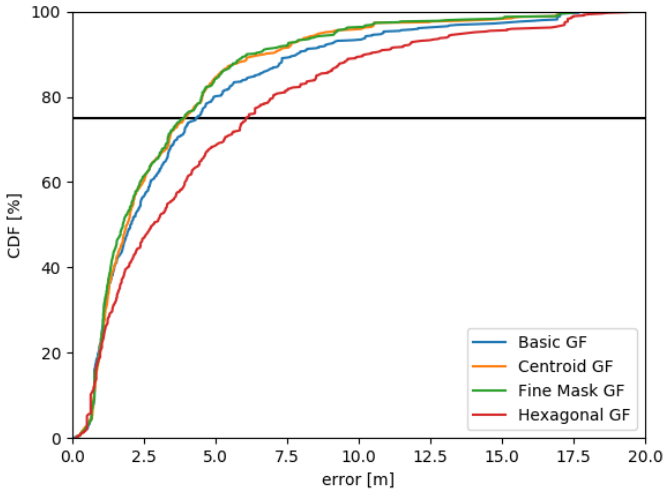

Fig. 12: Comparison of cumulative density functions (CDF) based on all errors for four grid-based methods with various configurations.

5.3 Shopping Mall - IPIN 2018 Competition

Fig. 13: The shopping mall scenario in France with multiple floors, wide corridors and visitors.

The IPIN 2018 competition took place in the shopping mall Atlantis le Centre (Figure 13) near Nantes, France (Boulevard Salvador Allende, 44800 Saint-Herblain, France). Organizers of the competition provided the dataset for the testing and the

validation of localisation systems [104]. Renaudin et al. [5] describe more details about the organization of the competition, the approach descriptions used by competitors, and the discussion about the results. A total area of 9 000 m^2 was dedicated to the competition.

5.3.1 Experiments on Training Dataset

The dataset consists of testing and validation logfiles with sensor measurements and ground truth positions for checkpoints. Every logfile contains between 10 and 24 checkpoints. Moreover, a single file with no ground truth is provided for the purpose of the off-site competition. The training subset helps to configure and calibrate competitor systems. In our case, the major part of testing was performed on the fourth testing path (T04_01 file). The path is more than 220 m long which is more than the scenario in the faculty building. The path consists of a straight walk, 90° turn to a wider corridor, a turnover and a returning to the initial position. The turnover and finish positions are placed in wide corridors not close to walls, which supports the evaluation of proposed methods and configurations, i.e., the parameter configuration is more important because the building structure does not help to detect the true position, especially at the end of the walk.

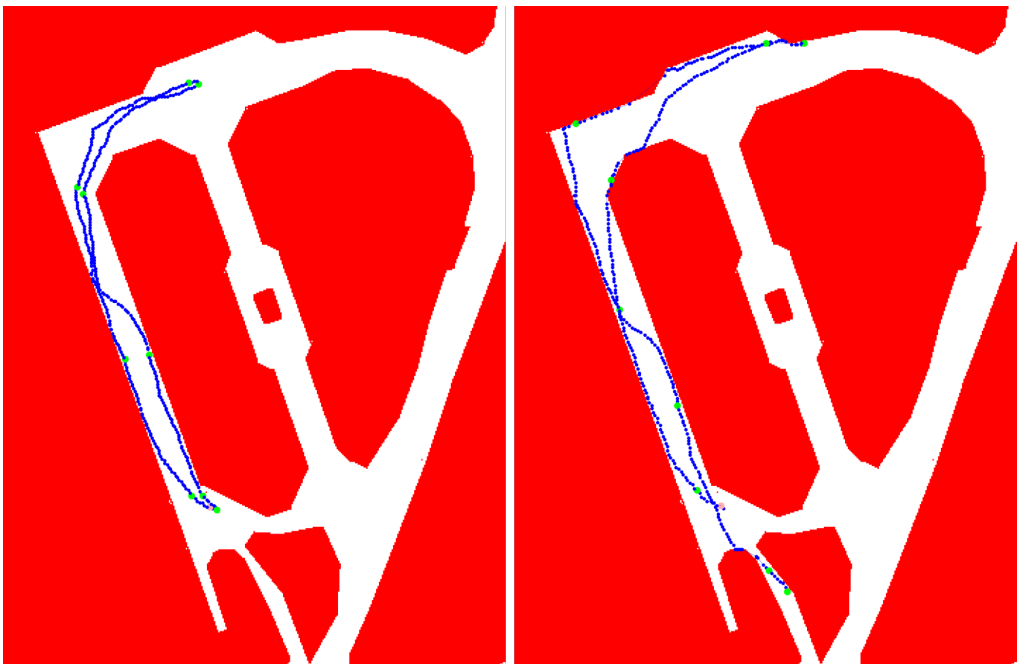

Fig. 14: Trajectories of estimated positions for the step length 70 cm (left figure) which achieved the third quartile of error 1.9 m and the step length 90 cm (right figure) with the error 21.8 m. The fine mask GF was applied with step SD = 5 cm and turn SD = 25 cm.

All observations from the faculty building were confirmed in this larger scenario. The loss of position occurs more often but with the same constraints. The third quartile of errors based on the T04 path ranges from 1.9 m to 28.5 m for different configurations. The real step length is unknown. Experiments with the final error greater than 8 m have tendencies to gain the maximal error at the finish position (typically for 80 cm and 90 cm step lengths). Other trials with more satisfactory accuracy produce the maximal error near the turnover. The user step length is unknown but the analysis demonstrates that the true step length is probably 65 cm (Figure 15). Averages of all distances between two consecutive steps on a single path were matched with the third quartile error of selected paths. However, the proper configuration for the unknown step length is not straightforward, even though it is possible to estimate this value by multiple runs with various settings.

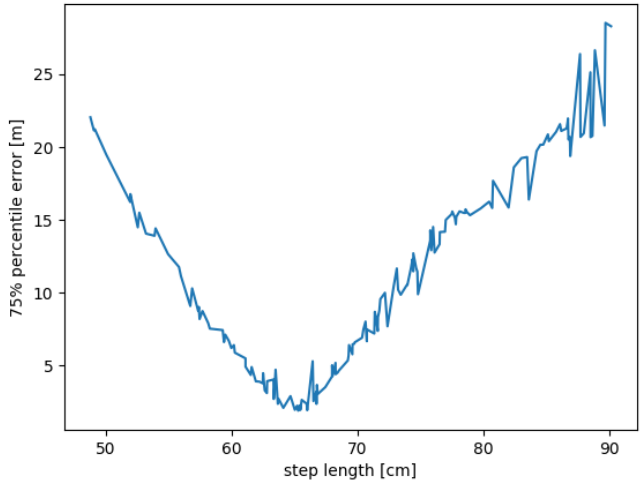

Fig. 15: The mean of all distances between two consecutive position estimations is portrayed with the respective third quartile of the error.

5.3.2 Evaluation on Validation Dataset

In total, 13 logfiles for 6 paths are provided as a validation dataset. A few different configurations were selected for all considered methods but with respect to the observations and recommended parameter settings. Table 2 describes the performance of the best configurations. The result is calculated as the third quartile of all errors for a single configuration among all paths. The best results for a single path was 2.3 m achieved by the fine mask GF and the hexagonal GF for same logfiles. Third quartiles of errors for single paths ranges from 2.3 m to 11.5 m with an exception of 37.7 m for the APM. The APM performance was not the worst. The best result was 2.6 m

Table 2: The best overall result for every considered method on the IPIN 2018 validation dataset.

Method	Result	Step Length	Step SD	Turn SD
Fine Mask GF	4.60 m	70 cm	15	30
Centroid GF	4.60 m	70 cm	15	30
Hexagonal GF	4.92 m	70 cm	10	10
Basic GF	5.11 m	65 cm	15	15
APM	5.30 m	65 cm	30	n/a
Particle Filter	6.18 m	65 cm	30	n/a

for the logfile V2.3 (best of all methods for that logfile). One of the main feature of the APM is the ability to track multiple paths and model the multimodal distribution using the multigrid approach. This features is mostly suitable, but in this case, the false trajectory gains the greater weight. The particle filter in such situations suppress these positions by resampling and grid filters cut off negligible values. Nevertheless, the APM is able to track multiple paths on a larger scale with wide corridors due to the ability to scale the grids and to cover large areas by reducing the precision. In this particular case, other grid filters achieved the error between 8.4 m and 9.4 m and the particle filter results in 7.9 m.

5.3.3 On-site Competition

Competitors were allowed to spend two days in the shopping mall. The first day was devoted to the survey of the area, improvement of the map model, and the calibration of the system. The second day was dedicated to the competition. Every participating team had two attempts. Two persons guided the competitor along the path with labels on the floor denoting the checkpoints. The competitor held the smartphone with the positioning application and provided the estimations for all checkpoints after the path was finished. The path consists of 70 checkpoints for the non-camera based on-site track. It was 840 m long including the parking lot, the outdoor area and corridors inside the shopping mall. Three different floors were included with the transitions using travelators and staircases. The competition event was during busy hours Saturday afternoon with lots of shopping mall visitors.

In our case, the centroidal GF was applied with step SD = 15 cm and turn SD = 15 cm. The first attempt failed due to the loss of position which was not handled properly in the application and caused by the underestimated step length. Smaller values for the step length achieved better results during the preliminary experiments in the

Table 3: The best results for considered methods on the IPIN 2018 on-site competition track. The mean, median, and 90th percentile are listed together with the third quartile of errors on 70 checkpoints.

Method	**75th**	**Mean**	**Median**	**90th**	**step l.**	**s. SD**	**t. SD**
Hexagonal GF	5.46 m	4.38 m	4.06 m	8.51 m	90 cm	5	5
Centroid GF	5.68 m	4.14 m	3.52 m	8.43 m	90 cm	5	15
APM	6.03 m	4.48 m	3.45 m	9.32 m	92 cm	44	n/a
Fine Mask GF	6.13 m	4.16 m	3.10 m	8.80 m	90 cm	25	25
Basic GF	6.37 m	4.60 m	3.74 m	9.21 m	90 cm	5	10
Particle Filter	7.00 m	4.79 m	3.65 m	9.33 m	88 cm	35	n/a

shopping mall. In the second attempt, the result was 37.5 m on the third quartile. One of the reasons of the error gain was faster pace and hence larger step lengths compared to the first attempt. Furthermore, the analysis of the results and more simulations on the recorded sensor measurements were performed.

Configurations for other experiments were systematically selected according to the previous recommendations. The goal of this analysis was to find the best possible configuration and to find the performance with the lowest error using the same system as during the on-site competition. The parameter values were selected randomly according to the given constraints. Table 3 describes the best obtained results. There were five performances out of 773 simulations which achieved the final third quartile error below 6 meters (2× hexagonal GF, 3× centroid GF). The average of the third quartiles for all used configurations are 27 m for fine mask GF, 26 m centroid GF, 31 m basic GF, and 35 m hexagonal GF. The particle filter reached 39 m and the APM 12 m (less configurations with underestimated step lengths were used for these two methods). Moreover, the trajectories of positions estimated by the APM have tendencies to match the real path more often on the largest straight segment (almost 200 m). The trajectory of other methods is often detected near the wall which was not the true path. The hexagonal GF achieved the best result of all. However, the median was the worst of all and the robustness of this method is worse compared to other approaches based also on other results (e.g., Figure 12).

The result of the best team in this on-site track was 5.5 m which is possible to obtain with the proposed system. In our case, the best results were achieved with small values of standard deviations. In real scenario, it is more beneficial to increase these values which leads to the worse accuracy but the system is more stable and robust to the sensor noise and step length estimations. The APM is observed to be the method providing the most stable satisfactory results considering various configurations.

5.4 Research Institute - IPIN 2019 Competition

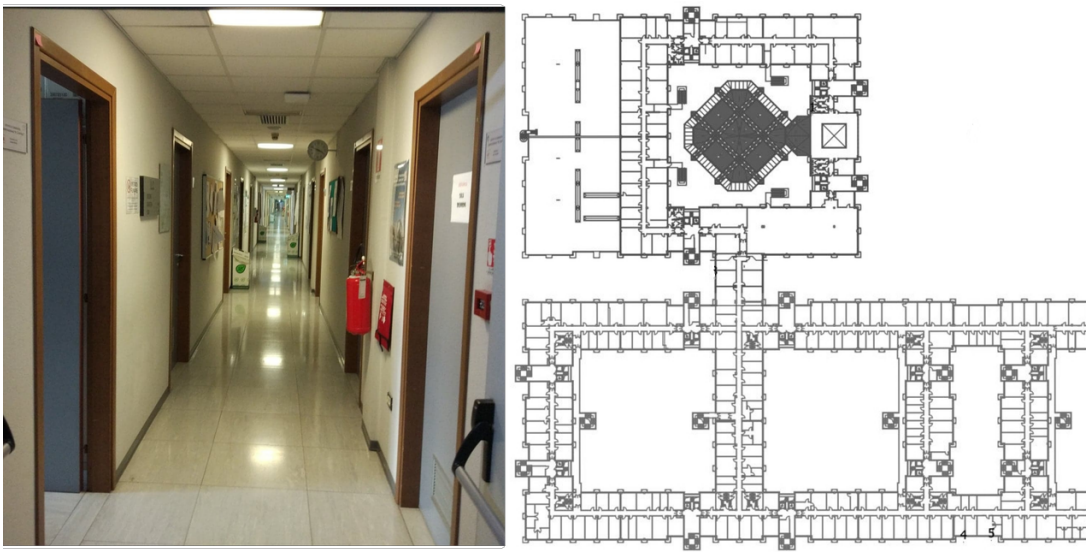

Fig. 16: The research institute in Italy with narrow corridors and multiple entry points to another floors (elevators and staircases) with the same appearance.

The IPIN 2019 competition took place in the research institute CNR Area of Pisa (Via Giuseppe Moruzzi, 56127 Pisa, Italy). Organizers of the competition provide the dataset for the testing and the validation of positioning systems [105]. Potorti et al. [6] describe the competition event organisation including the area mapping. Moreover, approaches used in the competition are introduced with the overall results discussion. A total area of 6 000 m^2 indoors and 1 000 m^2 outdoors was dedicated to the competition. The venue (Figure 16) differs from the shopping mall as its corridors are narrow and long and multiple directions are available on junctions. The presence of elevators and staircases, which have the same appearance and are close to each other, is the challenge also for the vertical localisation.

5.4.1 Evaluation on Validation Dataset

All proposed methods were examined on the validation dataset with no further calibration. Table 4 describes best results for the methods. Nine logfiles were available. The overall result is chosen as the third quartile of all errors grouped by the method configuration. Analysis of particular performances revealed observations, especially related to the particle filter and the APM. The third quartiles from single trials range between 1.3 m (achieved by the fine mask GF) to 25.5 m with two exceptions 57.9 m and 88.3 m for the particle filter. Significantly worse results are obtained for some more

complex multifloor paths. The particle filter often produced the trajectory which does not match the real path even with a zig-zag segments of position estimations. This implementation is not suitable for this type of building and the direction incorporation in the particle state may increase the overall performance of the method. The aforementioned feature of the APM to track multiple paths was the advantage in this scenario. The first validation logfile demonstrates the statement. The particle filter gets 88.3 m error, grid filters range from 17.1 to 25.8 m and the APM achieved 8.3 m. However, there are other situations where the APM does not outperformed other grid methods.

Table 4: The best overall result for every considered method on the IPIN 2019 validation dataset.

Method	**Result**	**Step Length**	**Step SD**	**Turn SD**
Fine Mask GF	6.23 m	70 cm	15	15
Hexagonal GF	7.09 m	70 cm	15	10
Centroid GF	7.27 m	70 cm	15	30
APM	7.49 m	70 cm	30	n/a
Particle Filter	8.01 m	70 cm	30	n/a
Basic GF	8.21 m	70 cm	15	15

5.4.2 On-site Competition

The on-site competition event was similar to the IPIN 2018 with the first day dedicated to the venue survey. However, during the competition, the actor held the competitor's device with the application. Therefore, it was not possible to calibrate the configuration for the expected step length. The competition path consists of three floors, 75 checkpoints, between 11 and 15 minutes in total including two breaks. The participation in the competition was unsuccessful. The application crashed and provided no position estimations after a few steps. According to the rules, the official third quartile error was 75.3 m.

The analysis of the results was performed to find the best possible performance using the same system. The aim on the on-site competition was to use centroid GF for the first attempt and possibly the APM for the second attempt. The path was retaken to obtain the sensor measurements for the analysis after the official competition since the crashed application provided no data. The error 143.8 m was obtained in that case. The main source of error was the floor transition. The detection of the transition was reliable but entry points (elevators and staircases) to the floor were close to each other. Instead of the resetting the filter with the initial position at a selected entry point according to the distance to the prior position, the filter should be initialized

with probabilities on all entry points. Using the proper transitions, the third quartile reduced from 143.8 m to 38.7 m. Improvement of the heading computation leaded to multiple results between 30 m and 40 m.

The another significant challenge was the transition between outdoors and indoors. Short segments between floor transitions did not gain as much error as the largest segment with lots of checkpoints and the path through the auditorium and the cafeteria. Utilizing the light sensor for the inside-outside transition detection reduced the error to 22.1 m. Multiple parameters were selected to achieve the best result 16.2 m. The result of the best team in this on-site track was 3.8 m. Despite the unsatisfactory result in this competition, the real drawbacks of the proposed system were revealed.

5.4.3 Off-site Competition

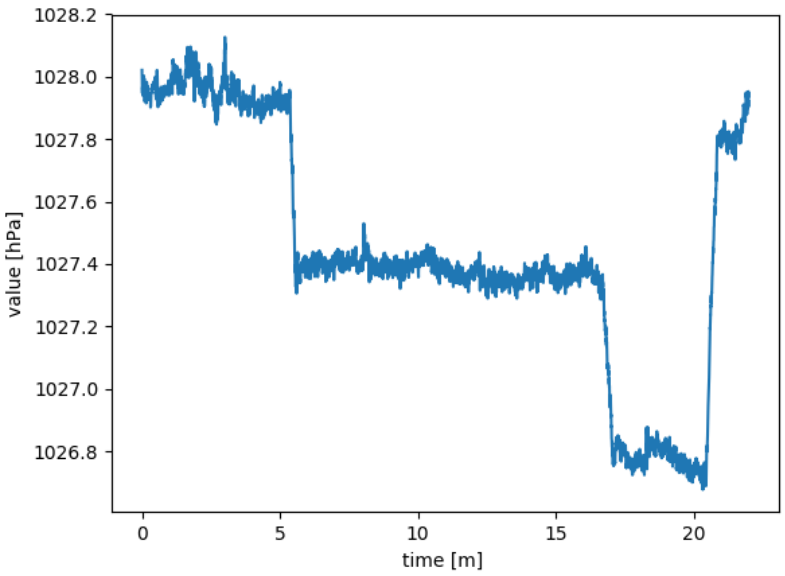

Fig. 17: Barometer values for the off-site track. Three different floors and transitions between them are recognizable.

The sensor measurements logfile was provided a few weeks before the on-site competition. The goal was to run the simulation and provide three attempts with two position estimations per second as no ground truth information was provided. The overall accuracy was calculated from these inputs. It takes more than 20 minutes for the actor to walk the path. Figure 17 visualizes the barometer measurements. The floor transitions are clearly visible. The path is also recognizable from the PDR or using any configuration. However, it is a challenge to obtain satisfactory result in this scenario.

Table 5: Official results for the off-site competition. The third quartile is the main criterion. Mean, median, 90th percentile and root mean square (RMS) values are listed.

Attempt	75th	Mean	Median	90th	RMS
First	7.0 m	4.0 m	1.7 m	9.1 m	6.0 m
Second	6.9 m	4.1 m	1.7 m	9.1 m	6.2 m
Third	6.6 m	3.9 m	2.0 m	9.1 m	5.8 m

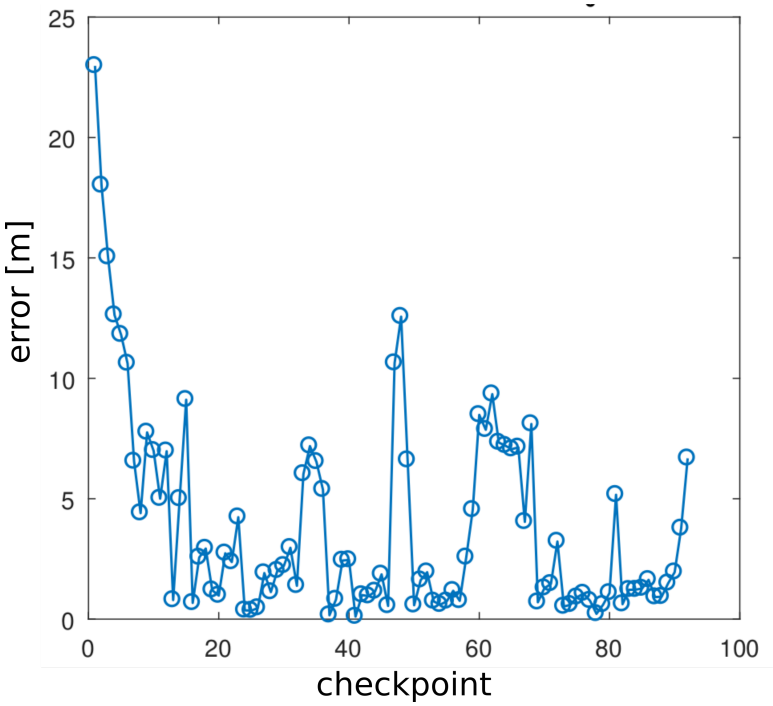

Fig. 18: Errors on all checkpoints in the off-site competition for the third attempt.

Table 5 demonstrates achieved results. The best team obtained the error 2.3 m. Compared to the on-site track, the main difference is that the initial position is not provided. The path started outdoors with GNSS available. Figure 18 portraits the errors along the path during the third attempt. The overall result is influenced by the inaccurate initial position. A few first checkpoints were outdoors along the 10 m wide corridor. Therefore, the map model was not able to reduce the error significantly in the beginning.

5.5 Discussion of Results and Lessons Learned

The evaluation verified the applicability of the proposed system. The fine mask GF and the centroid GF, as extensions of the basic GF, are the improvement of the

referenced method based on the evaluation results. The hexagonal grid filter was not elaborated further in terms of the convolution mask. Nevertheless, the filter outperformed other filters in some situations, especially considering the third quartile of errors criterion. However, the filter is not as robust and produced worse results for various inaccurate configurations. The observation is that better performance is obtained with overestimated step lengths and the greater error is gained for underestimated step lengths compared to other approaches.

The particle filter was implemented with the aim to compare it with grid-based filters. Mostly, it gained the greatest error among all proposed methods. However, better outcome is possible to obtain with improved versions of the filter and its features as declared by related work and the general tendency to use the particle filter for the indoor positioning. The advanced point-mass filter overcame the main drawbacks of grid-based filters and demonstrated the ability to follow the true trajectory of the user with its estimations. However, more parameters are included in the filter making it more difficult to configure the proper configuration.

The participation in IPIN competitions revealed advantages and drawbacks of proposed solutions. It is not trivial task to setup the conditions for such evaluation in local buildings of researchers, especially the mapping part. The benefit of the evaluation is also that it provides an insight into the real accuracy of the method and into other aspects, e.g., the reliability, which is valuable for the deployment of the application. This phenomenon is discussed for the IPIN 2018 on-site competition where the best result was obtained with less robust configurations and hence not suitable for the real positioning.

Related published papers devoted to the indoor positioning often declare high accuracy. However, the evaluation is often composed only in a single building, sometimes only a single path is taken and does not test other aspects of the solution. The contribution of such research effort is relevant for the field of positioning but the comprehensive comparison with related work is missing.

The experience based on the participation in competitions brings also ideas for the venue survey, the map model construction, the method calibration, and the parameter settings which is beneficial also for the new research, evaluation, or the application deployment. Moreover, it is possible to compare the systems, estimate the possible accuracy achievable with the proposed approach, and indicate the most suitable methods or their combinations.

The robustness of the application is challenged also with every new building. Considering this approach developed and tested in the faculty building, the expectations might be that the higher accuracy would be achieved in the research institute building

with narrow corridors than in the shopping mall with more freedom in movement. However, the presence of elevators, staircases, and multiple options on junctions produced greater errors and enforced the improvement of the applied approach.

Even though the general solution is needed for indoor positioning, the method may be adapted for the selected building. The research institute in Pisa contains double fire doors separating corridors and areas with elevators and staircases. The magnetometer-based solutions may be influenced by these doors and suffer in these regions but it also may be utilized for the door transition detection. Another example are two parallel corridors only about seven meters apart. It is challenging on the parameter configuration to distinguish the true corridor as it is possible to walk 250 m straight corridor and then turn into one of these two parallel corridors. However, one of them is outdoors (a balcony) which enables to utilize the light sensor to recognize the true path. Nevertheless, these approaches are not applicable in every building, e.g., the shopping mall have partially glass roof. Survey of the building in addition to detailed floor plans and the knowledge of the users may lead to the better experience of the positioning and navigation.

In PDR-based solutions, the error is increasing with every iteration. Using Bayesian filtering, the transition stage increase the uncertainty, which is reduced by the measurement in the evaluation stage. Besides the map model and floor transition, other landmarks may improve the performance. Possible landmarks are indoor-outdoor transitions, detection of activities, or landmarks using Wi-Fi, specific images from camera. Competitors (IPIN 2019) shared the idea that the future of indoor positioning is in combination of multiple complementary technologies [6].

Conclusion

In this thesis, the indoor positioning system was proposed. The smartphone-oriented solution is based on the pedestrian dead reckoning with the contribution of the map model. The Bayes filtering is the essential component of the introduced approach. Various Bayes filter implementations were examined, especially with focus on the grid-based methods. Unlike the commonly used particle filter, grid filters are deterministic and utilize the convolution for the system state computation. Besides the referenced particle filter, five Bayes filters based on two-dimensional grids were introduced. The basic grid filter tessellates the map into a regular square-shaped grid. The hexagonal grid, as an alternative, uses hexagonal grid to cover the space. The fine mask grid filter elaborates the basic grid filter with the improved convolution mask calculation. Moreover, the centroid grid filter utilizes the similar approach of two layers of grids and determines the so-called centroids of grid cells as estimated positions. The proposed adapted version of the advanced point-mass filter is using multigrid design with rotating and scaling grids. The APM connects advantages of various filter implementations as the convolution and the ability to focus on selected area as the particle filter does.

The evaluation was performed in three buildings. The single path in the faculty building was composed for the validation of proposed methods and to acquire general observations in known environment. The on-site track of the IPIN 2018 competition in the shopping mall and the provided dataset tested the system in the complex realistic scenario. The participation in the IPIN 2019 on-site and off-site competition in the research institute revealed weaknesses of the proposed implementation. More than 3 000 simulations were performed on given sensor measurements with the various configurations. The best results for grid-based methods were obtained between 4.6 m and 5.3 m for the validation dataset of the IPIN 2018 competition and between 6.2 m and 8.2 m for the IPIN 2019 competition validation dataset. The result of the IPIN 2018 on-site competition was 37.5 m using the centroid GF but the investigation led to the configurations with the third quartile of error between 5.5 m and 6.4 m. The IPIN 2019 off-site competition result was 6.6 m. The performance on the on-site track was unsuccessful and the further analysis led to the improvements achieving the error 16.2 m.

The proposed system is applicable considering the given use case. Nevertheless, some of approach weaknesses were identified and labeled for the improvement. Alternative implementations of the Bayesian filtering (especially extended versions of the particle filter), advanced map model (using probabilities instead of only accessibility Boolean value), and the sensor fusion are promising topics from the research point of view. To enhance the overall accuracy and stability of the proposed system, particular methods should be refined, e.g., the step length estimation or the floor transition including the initial position determination. Incorporation of an additional method may be needed for the significant improvement of the approach and clearly necessary for the deployment of the indoor navigation application. Besides the positioning module, the application needs the stable and robust implementation of the navigation and the visualisation of the map, the position, and the navigation signs. The real usage of the application will probably reveal more challenges.

Resumé

Práca sa venuje oblasti navigácie v indoor prostredí so zameraním na určenie aktuálnej polohy používateľa. Prezentované riešenie využíva smartfóny so zabudovanými senzormi. Spolu s modelom mapy aktuálneho poschodia je vypočítaná aktuálna pozícia v budove. Nepresnosti sú spôsobené šumom v meraniach zo senzorov a z nepresných odhadov aktuálneho natočenia a dĺžky kroku. Bayesovské filtrovanie dokáže modelovať tieto nepresnosti a poskytuje údaj o aktuálnom stave na základe pravdepodobností.

V tomto výskume sú prezentované viaceré implementácie bayesovského filtrovania využívajúce mriežku. Body (zodpovedajúce stredom políčok v mriežke) sú fixne umiestnené na mape tvoriac štvorcovú alebo šesťuholníkovú mriežku. Vylepšené verzie používajú dve úrovne mriežok na výpočet konvolučnej masky alebo aktuálnej pozície v rámci jedného políčka mriežky. Existujúci APM filter, ktorý dosiahol sľubné výsledky v porovnaní s často používaným časticovým filtrom, je prispôsobený na indoor lokalizáciu. Táto implementácia potláča slabé stránky mriežkových filtrov s využitím viacerých mriežok schopných sa otáčať a škálovať podľa potreby.

Prezentované prístupy sú overené v troch budovách. V budove fakulty bol realizovaný experiment na jednoduchej trase podporený video analýzou. Viaceré všeobecné pozorovania, nastavenia parametrov a použiteľnosť rôznych verzií filtrov boli predmetom záujmu. Datasety a priama účasť na súťaži IPIN 2018 v obchodnom dome vo Francúzsku ukázala silné stránky a slabiny prezentovaného riešenia. Použiteľnosť a univerzálnosť jednotlivých metód bola overená aj na datasetoch a v dvoch kategóriach na súťaži IPIN 2019 v budove výskumného inštitútu v Taliansku.

References

[1] Opiela, M. Indoor localization using accelerometer and compass. Master's Thesis, Košice: P. J. Šafárik University, 2015.

[2] Galčík, F., and Opiela, M. Grid-based indoor localization using smartphones. In *2016 International Conference on Indoor Positioning and Indoor Navigation (IPIN)* (oct 2016), IEEE, pp. 1–8.

[3] Opiela, M., and Galčík, F. Grid-based bayesian filtering methods for pedestrian dead reckoning indoor positioning using smartphones. *Sensors 20*, 18 (2020), 5343.

[4] Opiela, M. Indoor Localization based on Advanced Point-Mass Filtering Method. In *SOFSEM 2019: Theory and Practice of Computer Science : 45th International Conference on Current Trends in Theory and Practice of Computer Science : Proceedings of Student Research Forum.* (2019), Cham : Springer Nature, pp. 39–50.

[5] Renaudin, V., Ortiz, M., Perul, J., Torres-Sospedra, J., Jiménez, A. R., Pérez-Navarro, A., Mendoza-Silva, G. M., Seco, F., Landau, Y., Marbel, R., Ben-Moshe, B., Zheng, X., Ye, F., Kuang, J., Li, Y., Niu, X., Landa, V., Hacohen, S., Shvalb, N., Lu, C., Uchiyama, H., Thomas, D., Shimada, A., Taniguchi, R., Ding, Z., Xu, F., Kronenwett, N., Vladimirov, B., Lee, S., Cho, E., Jun, S., Lee, C., Park, S., Lee, Y., Rew, J., Park, C., Jeong, H., Han, J., Lee, K., Zhang, W., Li, X., Wei, D., Zhang, Y., Park, S. Y., Park, C. G., Knauth, S., Pipelidis, G., Tsiamitros, N., Lungenstrass, T., Morales, J. P., Trogh, J., Plets, D., Opiela, M., Fang, S., Tsao, Y., Chien, Y., Yang, S., Ye, S., Ali, M. U., Hur, S., and Park, Y. Evaluating indoor positioning systems in a shopping mall: The lessons learned from the IPIN 2018 competition. *IEEE Access 7* (2019), 148594–148628.

[6] Potortì, F., Park, S., Crivello, A., Palumbo, F., Girolami, M., Barsocchi, P., Lee, S., Torres-Sospedra, J., Jimenez, A. R., Pérez-Navarro, A., Mendoza-Silva, G. M., Seco, F., Ortiz, M., Perul, J., Renaudin, V., Kang, H., Park, S., Lee, J. H., Park, C. G., Ha, J., Han, J., Park, C., Kim, K., Lee, Y., Gye, S., Lee, K., Kim, E., Choi, J., Choi, Y.-S., Talwar, S., Cho, S. Y., Ben-Moshe, B., Scherbakov, A., Antsfeld, L., Sansano-Sansano, E., Chidlovskii, B., Kronenwett, N., Prophet, S., Landau, Y., Marbel, R., Zheng, L., Peng, A., Lin, Z., Wu, B., Ma, C., Poslad, S., Selviah, D. R., Wu, W., Ma, Z., Zhang, W., Wei, D., Yuan, H., bang Jiang, J., Huang, S.-Y., Liu, J.-W., Su, K.-W., Leu, J.-S., Nishiguchi, K., Bousselham, W., Uchiyama, H., Thomas, D., Shimada, A., Taniguchi, R.-I., Cortés, V., Lungenstrass, T., Ashraf, I., Lee, C., Ali, M. U., Im, Y., Kim, G., Eom, J., Hur, S., Park, Y., Opiela, M., Moreira, A., Nicolau, M. J., Pendão, C., Silva, I., Meneses, F., Costa, A., Trogh, J., Plets, D., Chien, Y.-R., Chang, T.-Y., hau Fang, S., and Tsao, Y. The ipin 2019 indoor localisation competition - description and results. *IEEE Access 8* (2020), n/a. Accepted on 15 October 2020.

[7] Slovenkai, S. Motion detection using smartphone sensors in indoor environments. Bachelor's Thesis, Košice: P. J. Šafárik University, 2017.

[8] Šimková, B. Using augmented reality for indoor navigation. Bachelor's Thesis, Košice: P. J. Šafárik University, 2018.

[9] Rojek, P. Smartphone user activity recognition in indoor environment. Bachelor's Thesis, Košice: P. J. Šafárik University, 2019.

[10] Džama, J. Indoor localization using particle filter. Bachelor's Thesis, Košice: P. J. Šafárik University, 2019.

[11] Hviščˇ, T. Indoor navigation for smartphone users. Bachelor's Thesis, Košice: P. J. Šafárik University, 2020.

[12] Furfari, F., Crivello, A., Barsocchi, P., Palumbo, F., and Potortì, F. What is next for indoor localisation? taxonomy, protocols, and patterns for advanced location based services. In *2019 International Conference on Indoor Positioning and Indoor Navigation (IPIN)* (2019), IEEE, pp. 1–8.

[13] Potortì, F., Crivello, A., Barsocchi, P., and Palumbo, F. Evaluation of indoor localisation systems: Comments on the iso/iec 18305 standard. In *2018*

International Conference on Indoor Positioning and Indoor Navigation (IPIN) (2018), IEEE, pp. 1–7.

[14] Lymberopoulos, D., and Liu, J. The microsoft indoor localization competition: Experiences and lessons learned. *IEEE Signal Processing Magazine 34*, 5 (2017), 125–140.

[15] Potortì, F., Barsocchi, P., Girolami, M., Torres-Sospedra, J., and Montoliu, R. Evaluating indoor localization solutions in large environments through competitive benchmarking: The evaal-etri competition. In *2015 International Conference on Indoor Positioning and Indoor Navigation (IPIN)* (2015), IEEE, pp. 1–10.

[16] Villien, C., Frassati, A., and Flament, B. Evaluation of an indoor localization engine. In *2019 International Conference on Indoor Positioning and Indoor Navigation (IPIN)* (2019), IEEE, pp. 1–8.

[17] Mendoza-Silva, G. M., Torres-Sospedra, J., Potortì, F., Moreira, A., Knauth, S., Berkvens, R., and Huerta, J. Beyond euclidean distance for error measurement in pedestrian indoor location. *IEEE Transactions on Instrumentation and Measurement* (2020).

[18] Mautz, R. Indoor Positioning Technologies. *Institute of Geodesy and Photogrammetry, Department of Civil, Environmental and Geomatic Engineering, ETH Zurich*, February 2012 (2012), 127.

[19] Al-Ammar, M. A., Alhadhrami, S., Al-Salman, A., Alarifi, A., Al-Khalifa, H. S., Alnafessah, A., and Alsaleh, M. Comparative survey of indoor positioning technologies, techniques, and algorithms. In *2014 International Conference on Cyberworlds* (2014), IEEE, pp. 245–252.

[20] Holcer, S., Torres-Sospedra, J., Gould, M., and Remolar, I. Privacy in indoor positioning systems: A systematic review. In *2020 International Conference on Localization and GNSS (ICL-GNSS)* (2020), IEEE, pp. 1–6.

[21] Barsocchi, P., Calabrò, A., Crivello, A., Daoudagh, S., Furfari, F., Girolami, M., and Marchetti, E. A privacy-by-design architecture for indoor localization systems. In *International Conference on the Quality of Information and Communications Technology* (2020), Springer, pp. 358–366.

[22] Han, D., Jung, S., Lee, M., and Yoon, G. Building a practical wi-fi-based indoor navigation system. *IEEE Pervasive Computing 13*, 2 (apr 2014), 72–79.

[23] Chumkamon, S., Tuvaphanthaphiphat, P., and Keeratiwintakorn, P. A blind navigation system using RFID for indoor environments. *2008 5th International Conference on Electrical Engineering/Electronics, Computer, Telecommunications and Information Technology* (may 2008), 765–768.

[24] Yang, J., Wang, Z., and Zhang, X. An iBeacon-based Indoor Positioning Systems for Hospitals. *International Journal of Smart Home 9*, 7 (2015), 161–168.

[25] Tiemann, J., and Wietfeld, C. Scalable and precise multi-UAV indoor navigation using TDOA-based UWB localization. In *2017 International Conference on Indoor Positioning and Indoor Navigation, IPIN 2017* (2017), vol. 2017-Janua, pp. 1–7.

[26] Bitsch Link, J. A., Gerdsmeier, F., Smith, P., and Wehrle, K. Indoor navigation on wheels (and on foot) using smartphones. In *2012 International Conference on Indoor Positioning and Indoor Navigation, IPIN 2012 - Conference Proceedings* (nov 2012), IEEE, pp. 1–10.

[27] Fetzer, T., Ebner, F., Bullmann, M., Deinzer, F., and Grzegorzek, M. Smartphone-Based Indoor Localization within a 13th Century Historic Building. *Sensors 18*, 12 (nov 2018), 4095.

[28] Wagner, J., Isert, C., Purschwitz, A., and Kistner, A. Improved vehicle positioning for indoor navigation in parking garages through commercially available maps. In *2010 International Conference on Indoor Positioning and Indoor Navigation, IPIN 2010 - Conference Proceedings* (sep 2010), IEEE, pp. 1–8.

[29] Scholz, M., Riedel, T., and Decker, C. A flexible architecture for a robust indoor navigation support device for firefighters. In *INSS 2010 - 7th International Conference on Networked Sensing Systems* (jun 2010), IEEE, pp. 227–232.

[30] Lin, Y.-H., Liu, Y.-S., Gao, G., Han, X.-G., Lai, C.-Y., and Gu, M. The ifc-based path planning for 3d indoor spaces. *Advanced Engineering Informatics 27*, 2 (2013), 189–205.

[31] Zhou, X., Xie, Q., Guo, M., Zhao, J., and Wang, J. Accurate and efficient indoor pathfinding based on building information modelling data. *IEEE Transactions on Industrial Informatics* (2020).

[32] Li, K.-J., Zlatanova, S., Torres-Sospedra, J., Pérez-Navarro, A., Laoudias, C., and Moreira, A. Survey on indoor map standards and formats.

In *2019 International Conference on Indoor Positioning and Indoor Navigation (IPIN)* (2019), IEEE, pp. 1–8.

[33] Pipelidis, G., Rad, O. R. M., Iwaszczuk, D., Prehofer, C., and Hugentobler, U. Dynamic vertical mapping with crowdsourced smartphone sensor data. *Sensors (Switzerland) 18*, 2 (feb 2018), 480.

[34] Möller, A., Kranz, M., Huitl, R., Diewald, S., and Roalter, L. A mobile indoor navigation system interface adapted to vision-based localization. In *Proceedings of the 11th international conference on mobile and ubiquitous multimedia* (2012), pp. 1–10.

[35] Rehman, U., and Cao, S. Augmented-reality-based indoor navigation: A comparative analysis of handheld devices versus google glass. *IEEE Transactions on Human-Machine Systems 47*, 1 (2016), 140–151.

[36] Kim, J., and Jun, H. Vision-based location positioning using augmented reality for indoor navigation. *IEEE Transactions on Consumer Electronics 54*, 3 (2008), 954–962.

[37] Petrelli, D., and O'Brien, S. Phone vs. tangible in museums: A comparative study. In *Proceedings of the 2018 CHI Conference on Human Factors in Computing Systems* (2018), pp. 1–12.

[38] Callebaut, G., Ottoy, G., and De Strycker, L. Bring your own sensor: Use your android smartphone as a sensing platform. In *2019 IEEE Sensors Applications Symposium (SAS)* (2019), IEEE, pp. 1–5.

[39] Stisen, A., Blunck, H., Bhattacharya, S., Prentow, T. S., Kjærgaard, M. B., Dey, A., Sonne, T., and Jensen, M. M. Smart Devices are Different: Assessing and Mitigating Mobile Sensing Heterogeneities for Activity Recognition. *Proceedings of the 13th ACM Conference on Embedded Networked Sensor Systems - SenSys '15* (2015), 127–140.

[40] Li, F., Zhao, C., Ding, G., Gong, J., Liu, C., and Zhao, F. A reliable and accurate indoor localization method using phone inertial sensors. *ACM Conference on Ubiquitous Computing (UbiComp)* (2012), 421–430.

[41] Blum, J. R., Greencorn, D. G., and Cooperstock, J. R. Smartphone Sensor Reliability for Augmented Reality Applications. In *International Conference on Mobile and Ubiquitous Systems: Computing, Networking, and Services* (dec 2013), Springer, Berlin, Heidelberg, pp. 127–138.

[42] Xu, Q., Zheng, R., and Hranilovic, S. IDyLL: indoor localization using inertial and light sensors on smartphones. In *Proceedings of the 2015 ACM International Joint Conference on Pervasive and Ubiquitous Computing - UbiComp '15* (New York, New York, USA, 2015), ACM Press, pp. 307–318.

[43] Mendoza-Silva, G. M., Torres-Sospedra, J., and Huerta, J. A meta-review of indoor positioning systems. *Sensors 19*, 20 (2019), 4507.

[44] Davidson, P., and Piché, R. A survey of selected indoor positioning methods for smartphones. *IEEE Communications Surveys & Tutorials 19*, 2 (2016), 1347–1370.

[45] Wang, J. Pseudolite applications in positioning and navigation: Progress and problems. *Journal of Global Positioning Systems 1*, 1 (2002), 48–56.

[46] Tariq, Z. B., Cheema, D. M., Kamran, M. Z., and Naqvi, I. H. Non-gps positioning systems: A survey. *ACM Computing Surveys (CSUR) 50*, 4 (2017), 1–34.

[47] Torres-Sospedra, J., Montoliu, R., Trilles, S., Belmonte, Ó., and Huerta, J. Comprehensive analysis of distance and similarity measures for wi-fi fingerprinting indoor positioning systems. *Expert Systems with Applications 42*, 23 (2015), 9263–9278.

[48] Rai, A., Chintalapudi, K. K., Padmanabhan, V. N., and Sen, R. Zee: zero-effort crowdsourcing for indoor localization. In *Proceedings of the 18th annual international conference on Mobile computing and networking - Mobicom '12* (New York, New York, USA, 2012), ACM Press, p. 293.

[49] He, S., and Chan, S.-H. G. Wi-fi fingerprint-based indoor positioning: Recent advances and comparisons. *IEEE Communications Surveys & Tutorials 18*, 1 (2015), 466–490.

[50] Khalajmehrabadi, A., Gatsis, N., and Akopian, D. Modern wlan fingerprinting indoor positioning methods and deployment challenges. *IEEE Communications Surveys & Tutorials 19*, 3 (2017), 1974–2002.

[51] Kriz, P., Maly, F., and Kozel, T. Improving Indoor Localization Using Bluetooth Low Energy Beacons. *Mobile Information Systems 2016* (apr 2016), 1–11.

[52] Karmacharya, A., Silva, G. M. M., and Torres-Sospedra, J. Sensor fusion and well-conditioned triangle approach for ble-based indoor positioning. In *Proceedings of the International Conference on Localization and GNSS (ICL-GNSS 2020), Tampere, Finland, June 2nd to 4th, 2020 - Work in Progress Papers* (2020), vol. 2626 of *CEUR Workshop Proceedings*.

[53] Alarifi, A., Al-Salman, A., Alsaleh, M., Alnafessah, A., Al-Hadhrami, S., Al-Ammar, M. A., and Al-Khalifa, H. S. Ultra wideband indoor positioning technologies: Analysis and recent advances. *Sensors 16*, 5 (2016), 707.

[54] Solin, A., Kannala, J., and Rahtu, E. Terrain Navigation in the Magnetic Landscape : Particle Filtering for Indoor Positioning.

[55] Biswas, J., and Veloso, M. WiFi localization and navigation for autonomous indoor mobile robots. In *Proceedings - IEEE International Conference on Robotics and Automation* (2010), pp. 4379–4384.

[56] Goyal, P., Ribeiro, V. J., Saran, H., and Kumar, A. Strap-down Pedestrian Dead-Reckoning system. In *2011 International Conference on Indoor Positioning and Indoor Navigation, IPIN 2011* (sep 2011), IEEE, pp. 1–7.

[57] Skog, I., Nilsson, J.-O., and Händel, P. Evaluation of zero-velocity detectors for foot-mounted inertial navigation systems. In *2010 International Conference on Indoor Positioning and Indoor Navigation, IPIN 2010 - Conference Proceedings* (sep 2010), IEEE, pp. 1–6.

[58] Jimenez, A. R., Seco, F., Prieto, J. C., and Guevara, J. Indoor Pedestrian navigation using an INS/EKF framework for yaw drift reduction and a foot-mounted IMU. In *Proceedings of the 2010 7th Workshop on Positioning, Navigation and Communication, WPNC'10* (mar 2010), IEEE, pp. 135–143.

[59] Bergmann, J., and Hou, X. Pedestrian dead reckoning with wearable sensors: a systematic review. *IEEE Sensors Journal* (2020).

[60] Wu, Y., Zhu, H.-B., Du, Q.-X., and Tang, S.-M. A survey of the research status of pedestrian dead reckoning systems based on inertial sensors. *International Journal of Automation and Computing 16*, 1 (2019), 65–83.

[61] Zhang, Y., Liu, W., Yang, X., and Xing, S. Hidden markov model-based pedestrian navigation system using MEMS inertial sensors. *Measurement Science Review 15*, 1 (jan 2015), 27–34.

[62] Brajdic, A., and Harle, R. Walk detection and step counting on unconstrained smartphones. *Proceedings of the 2013 ACM international joint conference on Pervasive and ubiquitous computing - UbiComp '13* (2013), 225.

[63] Lee, H. H., Choi, S., and Lee, M. J. Step detection robust against the dynamics of smartphones. *Sensors (Switzerland) 15*, 10 (oct 2015), 27230–27250.

[64] Link, J. Á. B., Smith, P., Viol, N., and Wehrle, K. FootPath: Accurate map-based indoor navigation using smartphones. In *2011 International Conference on Indoor Positioning and Indoor Navigation, IPIN 2011* (sep 2011), IEEE, pp. 1–8.

[65] Radu, V., and Marina, M. K. HiMLoc: Indoor smartphone localization via activity aware pedestrian dead reckoning with selective crowdsourced WiFi fingerprinting. In *2013 International Conference on Indoor Positioning and Indoor Navigation, IPIN 2013* (oct 2013), IEEE, pp. 1–10.

[66] Vezocnik, M., and Juric, M. B. Average Step Length Estimation Models' Evaluation Using Inertial Sensors: A Review, jan 2018.

[67] Weinberg, H. Using the ADXL202 in pedometer and personal navigation applications. Tech. rep., 2002. www.BDTIC.com/ADI http://application-notes.digchip.com/013/13-14984.pdf, accessed on 15 July 2020.

[68] Tian, Q., Salcic, Z., Wang, K. I.-K., and Pan, Y. A Multi-Mode Dead Reckoning System for Pedestrian Tracking Using Smartphones. *IEEE Sensors Journal 16*, 7 (apr 2016), 2079–2093.

[69] Wang, H., Elgohary, A., and Choudhury, R. R. No Need to War-Drive : Unsupervised Indoor Localization. *Proceedings of the 10th international conference on Mobile systems, applications, and services (MobiSys '12)* (2012), 197–210.

[70] Ettlinger, A., Neuner, H., and Burgess, T. Development of a Kalman filter in the Gauss-Helmert model for reliability analysis in orientation determination with smartphone sensors. *Sensors (Switzerland) 18*, 2 (jan 2018), 414.

[71] Wu, D., Xia, L., and Geng, J. Heading estimation for pedestrian dead reckoning based on Robust adaptive Kalman filtering. *Sensors (Switzerland) 18*, 6 (jun 2018), 1970.

[72] Kang, W., Nam, S., Han, Y., and Lee, S. Improved heading estimation for smartphone-based indoor positioning systems. In *IEEE International Symposium on Personal, Indoor and Mobile Radio Communications, PIMRC* (sep 2012), IEEE, pp. 2449–2453.

[73] Seo, J., and Laine, T. H. Accurate position and orientation independent step counting algorithm for smartphones. *Journal of Ambient Intelligence and Smart Environments 10*, 6 (nov 2018), 481–495.

[74] Bojja, J., Kirkko-Jaakkola, M., Collin, J., and Takala, J. Indoor localization methods using dead reckoning and 3D map matching. *Journal of Signal Processing Systems 76*, 3 (2014), 301–312.

[75] Chen, Z., Zou, H., Jiang, H., Zhu, Q., Soh, Y. C., and Xie, L. Fusion of WiFi, smartphone sensors and landmarks using the kalman filter for indoor localization. *Sensors 15*, 1 (jan 2015), 715–732.

[76] Xia, H., Wang, X., Qiao, Y., Jian, J., and Chang, Y. Using multiple barometers to detect the floor location of smart phones with built-in barometric sensors for indoor positioning. *Sensors (Switzerland) 15*, 4 (mar 2015), 7857–7877.

[77] Radu, V., Tong, C., Bhattacharya, S., Kawsar, F., Marina, M. K., Lane, N. D., and Mascolo, C. Multimodal Deep Learning for Activity and Context Recognition. *Proceedings of the ACM on Interactive, Mobile, Wearable and Ubiquitous Technologies 1*, 4 (2018), 1–27.

[78] Susi, M., Renaudin, V., and Lachapelle, G. Motion mode recognition and step detection algorithms for mobile phone users. *Sensors (Switzerland) 13*, 2 (jan 2013), 1539–1562.

[79] Hussain, G., Jabbar, M., Cho, J.-D., and Bae, S. Indoor Positioning System: A New Approach Based on LSTM and Two Stage Activity Classification. *Electronics 8*, 4 (mar 2019), 375.

[80] Wang, X., Yu, Z., and Mao, S. Deepml: Deep lstm for indoor localization with smartphone magnetic and light sensors. In *2018 IEEE International Conference on Communications (ICC)* (2018), IEEE, pp. 1–6.

[81] Wang, J., Chen, Y., Hao, S., Peng, X., and Hu, L. Deep learning for sensor-based activity recognition: A survey. *Pattern Recognition Letters 119* (2019), 3–11.

[82] Shao, W., Luo, H., Zhao, F., Ma, Y., Zhao, Z., and Crivello, A. Indoor positioning based on fingerprint-image and deep learning. *IEEE Access 6* (2018), 74699–74712.

[83] Li, J., Wang, C., Kang, X., and Zhao, Q. Camera localization for augmented reality and indoor positioning: A vision-based 3d feature database approach. *International Journal of Digital Earth* (2019).

[84] Duque Domingo, J., Gómez-García-Bermejo, J., Zalama, E., Cerrada, C., and Valero, E. Integration of computer vision and wireless networks to provide indoor positioning. *Sensors 19*, 24 (2019), 5495.

[85] Cooper, A., and Hegde, P. An indoor positioning system facilitated by computer vision. In *2016 IEEE MIT Undergraduate Research Technology Conference (URTC)* (2016), IEEE, pp. 1–5.

[86] Chen, Z. H. E. Bayesian Filtering: From Kalman Filters to Particle Filters, and Beyond. *Statistics 182*, 1 (2003), 1–69.

[87] Fox, D., and Hightower, J. Bayesian filtering for location estimation. *IEEE Pervasive Computing 2*, 3 (jul 2003), 24—-33.

[88] Renaudin, V., Demeule, V., and Ortiz, M. Adaptative pedestrian displacement estimation with a smartphone. In *2013 International Conference on Indoor Positioning and Indoor Navigation, IPIN 2013* (oct 2013), IEEE, pp. 1–9.

[89] Moder, T., Hafner, P., Wisiol, K., and Wieser, M. 3D indoor positioning with pedestrian dead reckoning and activity recognition based on Bayes filtering. In *IPIN 2014 - 2014 International Conference on Indoor Positioning and Indoor Navigation* (oct 2014), IEEE, pp. 717–720.

[90] Arulampalam, M., Maskell, S., Gordon, N., and Clapp, T. A tutorial on particle filters for online nonlinear/non-Gaussian Bayesian tracking. *IEEE Transactions on Signal Processing 50*, 2 (2002), 174–188.

[91] Gordon, N., Salmond, D., and Smith, A. *IEE Proceedings. Part F. Radar and signal processing*, vol. 140. Institution of Electrical Engineers, apr 1993.

[92] Isard, M., and Blake, A. CONDENSATION - Conditional Density Propagation for Visual Tracking. *International Journal of Computer Vision 29*, 1 (1998), 5–28.

[93] Xie, Z., Guan, W., Zheng, J., Zhang, X., Chen, S., Chen, B., Xie, Z., Guan, W., Zheng, J., Zhang, X., Chen, S., and Chen, B. A High-Precision, Real-Time, and Robust Indoor Visible Light Positioning Method Based on Mean Shift Algorithm and Unscented Kalman Filter. *Sensors 2019, Vol. 19, Page 1094 19*, 5 (mar 2019), 1094.

[94] Lu, C., Uchiyama, H., Thomas, D., Shimada, A., and Taniguchi, R. I. Indoor positioning system based on chest-mounted IMU. *Sensors (Switzerland) 19*, 2 (jan 2019), 420.

[95] Burgard, W., Fox, D., Hennig, D., and Schmidt, T. Position tracking with position probability grids. *Proceedings of the First Euromicro Workshop on Advanced Mobile Robots (EUROBOT '96)* (1996), 2–9.

[96] Herrero-Pérez, D., Martínez-Barberá, H., Leblanc, K., and Saffiotti, A. Fuzzy uncertainty modeling for grid based localization of mobile robots. *International Journal of Approximate Reasoning 51*, 8 (2010), 912–932.

[97] Xu, W., Liu, L., Zlatanova, S., Penard, W., and Xiong, Q. A pedestrian tracking algorithm using grid-based indoor model. *Automation in Construction 92* (2018), 173–187.

[98] Hafner, P., Moder, T., Wieser, M., and Bernoulli, T. Evaluation of smartphone-based indoor positioning using different Bayes filters. In *2013 International Conference on Indoor Positioning and Indoor Navigation, IPIN 2013* (oct 2013), IEEE, pp. 1–10.

[99] Ning, F.-S., and Chen, Y.-C. Combining a modified particle filter method and indoor magnetic fingerprint map to assist pedestrian dead reckoning for indoor positioning and navigation. *Sensors 20*, 1 (2020), 185.

[100] Landa, V., Ben-Moshe, B., Hacohen, S., and Shvalb, N. GoIn – An Accurate InDoor Navigation Framework for Mobile Devices. *2018 International Conference on Indoor Positioning and Indoor Navigation (IPIN)*, September (sep 2018), 5–6.

[101] Teammco, Richard and Xie, William. Activity-Based Indoor Localization with Smartphones. https://github.com/teammcr192/activity-indoor-localization, accessed on 21 May 2019.

[102] Šimandl, M., Královec, J., and Söderström, T. Advanced point-mass method for nonlinear state estimation. *Automatica 42*, 7 (2006), 1133–1145.

[103] Opiela, M. Supplementary evaluation files for the paper: Grid-Based Bayesian Filtering Methods for Pedestrian Dead Reckoning Indoor Positioning Using Smartphones, Aug. 2020. https://doi.org/10.5281/zenodo.3975389.

[104] Ruiz, A. R. J., Mendoza-Silva, G. M., Ortiz, M., Perez-Navarro, A., Perul, J., Seco, F., and Torres-Sospedra, J. Datasets and Supporting Materials for the IPIN 2018 Competition Track 3 (Smartphone-based, off- site), Apr. 2018. https://doi.org/10.5281/zenodo.2823964.

[105] Ruiz, A. R. J., Perez-Navarro, A., Crivello, A., Mendoza-Silva, G. M., Seco, F., Ortiz, M., Perul, J., and Torres-Sospedra, J. Datasets and Supporting Materials for the IPIN 2019 Competition Track 3 (Smartphone-based, off- site), Oct. 2019. https://doi.org/10.5281/zenodo.3606765.

List Of Appendices

INDORA - System Description

Miroslav Opiela
Institute of Computer Science, Faculty of Science, P.J. Šafárik University
Jesenná 5, 041 54 Košice, Slovak Republic
miroslav.opiela@upjs.sk

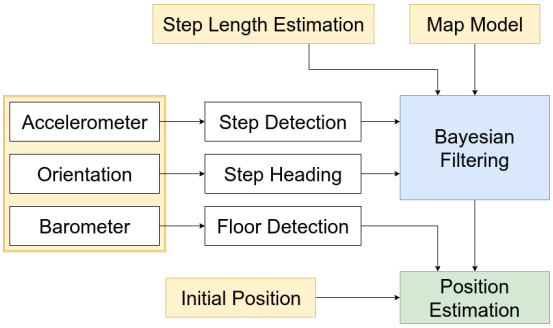

Fig. 1. Localization system overview. Sensor measurements processing, map model and grid-based bayesian filtering are the main components of the proposed positioning approach.

I. Introduction

Project INDORA originates from a few student research projects and final theses, especially the author's dissertation. Various bachelor and master theses have reviewed different aspects of a comprehensive indoor positioning system during recent years. Pedestrian dead-reckoning, map model and bayesian filtering are essential components of the proposed localization system (Figure 1). The main research focus is on a low-dimensional grid-based bayesian filtering, as a less elaborated alternative to Kalman and Particle filters widely used for the positioning. A semi-automatically generated map model helps to reduce the localization error introduced by noisy sensor measurements and inaccurate system configuration, e.g., a step length estimation. The considered use case involves a user with handheld smartphone. The system relies mostly on the map and no additional infrastructure is required in the building. The floor transition detection based on barometer measurements ensures the correct considered floor map and allows the localization system to estimate the user position only within the single floor.

The system foundations were specified in the author's master thesis (available only in Slovak). A software developed for the thesis was intended to be used as a prototype of the indoor localization and navigation application. However, the later stages of development were focused on the methods evaluation and IPIN competitions [2]. This paper summarizes the file formats, methods and software tools to handle the live smartphone-based positioning, data recording and localization results analysis.

II. Map Model

A building may consist of multiple maps. Typically, a single map corresponds to a single floor in the building. Moreover, a large floor may be split to more maps, especially when a limited amount of transition between these maps exist. The map model is constructed from floor plans using a map editor.

A. Indora Map Editor

A custom tool developed as a Java desktop application serves as a platform to create the map model.

Input, required for a single map, consists of the floor plan, the map scale (centimeters/pixel), a georeferenced position (WGS-84) of the initial point [0,0] in the image and the map rotation.

Multiple layers are generated for each map. The most important layer for the proposed approach is called base layer and it expresses the map model in terms of walls, doors and zones. Other layers capture positions of QR codes, map exitss (e.g., stairs, doors outside the building, elevators), key positions for the navigation, etc.

1) Base Layer: Points and connections are created using the map editor application. These elements are stored in a file, as a list of points (ID, x, y, type, description) and a list of connections (StartPointID, EndPointID, type, description). There are two types of points - simple points (represent single positions on the map) and zone points denoting positions of zones, i.e., closed areas bounded by connections. The description contains additional information about the zone, e.g., an assigned room. Rooms are used for the semantical representation of the map and may consist of multiple zones. Zones are elementary blocks composing the map. The automatic map export requires the zones to be convex polygons (it is verified by the application). There are three main types of connections - doors, walls (possibly with different width) and open connections. In case of nonconvex zone, the area should be split using one or more open connections to create convex zones.

2) Zone creation: A single zone is denoted as a point $Z[x_z, y_z]$ inside a convex polygon formed by n connections. The list of connections (or corresponding points) is automatically obtained from the annotated map. A first connection C_0C_1 of a zone is selected from a list of all connections such that there is an intersection between lines C_0C_1 and a vertical line ZZ_0, where $Z_0[x_z, 0]$ and Z is the zone point and the distance between the intersection and Z is minimal. Next point C_2 is selected from all connections from point $C1$ except

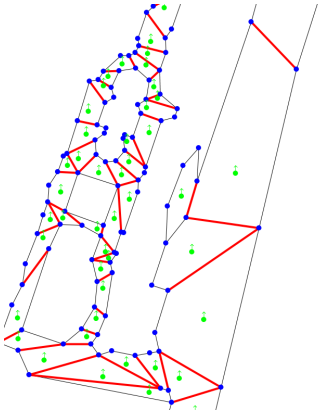

Fig. 2. Part of map from IPIN 2018 competition in shopping mall. Zones forming convex polygons are marked with green points. Walls are represented by blue lines. Red lines are doors or open connections.

C_0C_1. Connection C_1C_X is selected with the minimal angle $C_0C_1C_X$. The process repeats until the connection $C_{n-1}C_0$ is found.

The map editor supports easy annotation of the building with multiple features, e.g., an automatic points alignment along the line, zone completness, convex polygon rule and accessibility check (at least one of connections should be door or open).

3) Map model export: The map model is generated and exported in a binary file required by the localization application. The file format is defined as follows:

- List of simple points excluding zone points - x and y positions in centimeters.
- List of rooms with indices of corresponding zones.
- List of zones. For every zone, the description, a list of map points $C_0, C_1, \ldots, C_{n-1}$ and list of corresponding connection types is stored.

III. Indora Application

The application developed for Android OS provides indoor position estimations and it enables two modes - live localization with activated sensors and debug mode with deactivated sensors and simulation interface. The application is prepared to be extended for a full indoor navigation, but in this stage the UI/UX and other aspects of the proper application have a low priority.

1) Building representation: A single XML file describes common details about all maps composing the building, e.g., map names, sizes, rotations and scales. Each map includes a binary file for every layer exported from the map editor, the image file, which may be more user-friendly representation of the map compared to the floor plan and a single XML file with details regarding the map visualization. Data for the building are attached to the application as assets with a future possibility to download these files for the specified building.

2) Localization service: The localization method is implemented as a stand-alone service providing the location estimation on a single map, i.e., two-dimensional point $[x, y]$.

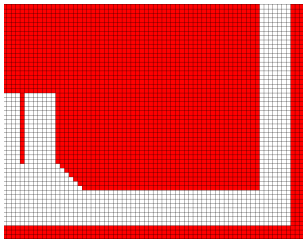

Fig. 3. Map tessellated into the grid. Every grid cell corresponds to the area $33 \times 33cm^2$. Red cells are inaccessible.

The grid-based bayesian filtering is the core component of the positioning using smartphone sensors for pedestrian dead-reckoning (PDR). Details regarding the implementation are available in a conference paper [1] and the localization system overview is included in journal paper describing the IPIN 2018 competition [2]. Bayesian filtering method probabilistically estimates the system state in two steps - prediction phase based on the PDR brings more uncertainty to the estimation and update phase utilizes the map model to adjust belief values for selected grid cells, i.e., invalid movement through walls and outside the accessible map area is restricted.

The application loads the base layer of the map model and creates a grid as an array of integer values where #0 is a value for accessible grid cells. The method for generating the grid is as follows:

- Set grid scale - centimeters per a grid cell and create the map grid (e.g., two-dimensional array) with predefined value for inaccessible grid cells (#1)
- Iterate over all connections for all zones. Place specified value for doors, open connections (#3) and walls (#2) using line drawing algorithm.
- Iterate over all zones. Starting from the zone point, use flood-fill algorithm to fill zone areas bounded by the marked connections with accessible values (#0).
- Mark all grid cells representing doors and open connections (#3) as accessible (#0).

3) Debug, recording, playback: The application is running in two modes. Live localization requires input with a map identifier and initial position coordinates. During evaluation, it is often obtained using QR codes or manually when only a single position is required (e.g., IPIN competition). Sensors are deactivated using the offline mode. The application may record raw sensor measurements according to the specified sensors and save them to a file in format similar to IPIN off-site competition, i.e. one line represents a single sensor measurement with timestamp, sensor identifier and relevant values. The file also contains a time synchronization event using NTP (Network Time Protocol) and marker events, i.e. when the button is pressed by the user. The initial position is typically inserted into the file manually afterwards.

The offline simulation and analysis is performed on real devices in a way that the file is scanned and sensor measurement or other events are triggered with respect to the timestamps. Therefore, the positioning system is forced to be running in

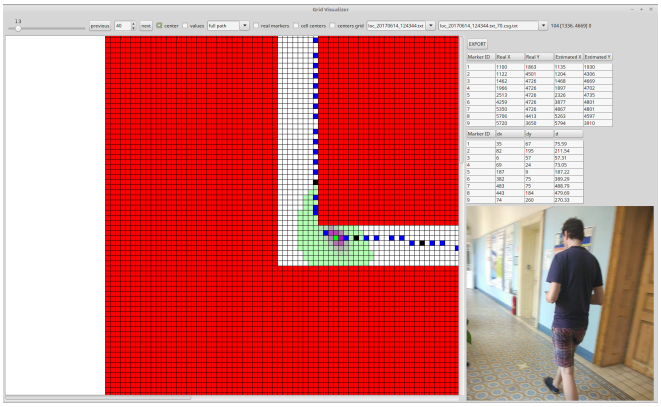

Fig. 4. Grid visualizer with interactive grid and camera capture. Blue squares forms the estimated path. Red and white cells denotes the accessibility of positions on the map. Green and purple colors are chosen to display the belief values of non-negligible grid cells.

real time. The condition for the real time computation is to finish the position estimation before the next step is detected. The motivation for such approach is the possibility to compare different localization methods and configurations on the same experiment.

Every method has various parameters which may be set for every attempt, e.g., method used, standard deviation for the step length estimation, step length value, number of particles in Particle filter, etc. These values may be selected in application settings menu when a recording is replayed. Moreover, playlists are composed as CSV files where every line represents a single playback with specified settings which are selected automatically. Therefore, it is possible to replay the same sensor measurements on a large amount of different configurations.

Output of a single run is a JSON file describing the positioning process. It includes the timestamp of the playback (it is also the filename), filename of the sensor recordings, method used, selected parameter values and JSON arrays with x, y coordinates, map identifiers and possibly the button pressed events for every position estimation performed when a step was detected. The file is used in offline non-android tools for comparing different methods and evaluating the localization system in general.

Proposed methods are analyzed offline. To support the recorded measurements with the camera image, an Android application was developed which enriches the video recording with a CSV file. In the file, a timestamp is matched to every video frame. Moreover, the timestamp is synchronized with NTP time to align the video. Typically, for every position when a step is detected, the corresponding frame is extracted from the video and stored separately.

IV. Grid Visualizer and Media Recorder

Grid visualizer application merges these inputs and provides a visual output. An interactive map grid is displayed with possibility to see belief values for different positions. The overall path, positions on checkpoints and camera image supports the general evaluation. This type of analysis is demanding on the file size. Therefore, when a large amount of different configuration is expected, JSON files are processed and instead of interactive map and camera captures, the output in form of images is provided. A single image corresponds to a single map where the positions along the detected path are marked. Calculated errors on the checkpoints are stored for the postprocessing and the main values, e.g., 75th percentile, are placed in the image. Depending on the map, the path is drawn on a map grid (useful for smaller scenarios) or original map picture (floor plan). Various particular script tools written in Python or Java are used for further results analysis and error visualization.

Currently, some of these tools are reviewed by bachelor or master students as a part of their final theses with possibility of the approach improvement or replacement.

References

[1] Galčík, František, and Miroslav Opiela. "Grid-based indoor localization using smartphones." 2016 International Conference on Indoor Positioning and Indoor Navigation (IPIN). IEEE, 2016.

[2] Renaudin, Valerie, et al. "Evaluating Indoor Positioning Systems in a Shopping Mall: The Lessons Learned From the IPIN 2018 Competition." IEEE Access 7 (2019): 148594-148628.